Piezotronics and piezo-phototronics for adaptive electronics and optoelectronics

Wenzhuo Wu[1,2] and Zhong Lin Wang[1,3]

Low-dimensional piezoelectric semiconductor nanomaterials, such as ZnO and GaN, have superior mechanical properties and can be integrated into flexible devices that can be subjected to large strain. More importantly, the coupling between piezoelectric polarization and semiconductor properties (for example, electronic transport and photoexcitation) in these materials gives rise to unprecedented device characteristics. This has increased research interest in the emerging fields of piezotronics and piezo-phototronics, which offer new means of manipulating charge-carrier transport, generation, recombination or separation in the controlled operation of flexible devices through the application of external mechanical stimuli. We review the recent progress in advancing our fundamental understanding and in realizing practical applications of piezotronics and piezo-phototronics, and provide an in-depth discussion of future research directions.

The seamless and adaptive interactions between functional devices and their environment (for example, the human body) are crucial for advancing emerging technologies, such as wearable electronics, robotics, the Internet of Things, biomedical engineering and human–machine interfacing[1,2]. Although mechanical signals are inherent in these applications, electrical manipulation of charge carriers is the important physical process in state-of-the-art semiconductor technology[3,4] and in emerging nanodevices[5–11]. Therefore, mechanical stimuli need to be converted to electrical signals to be sensed by and elicit a response from associated devices. This scheme of operation not only requires the complex integration of heterogeneous components, but also lacks a direct interaction between the (opto)electronic component and the external mechanical stimulus. These limitations have seriously hampered the advancement and broader use of electronics technologies to transduce mechanical signals.

Piezoelectric materials, which produce polarization under mechanical deformation, are widely used for electromechanical applications. Research in this area has been traditionally focused on bulk or thin-film ceramics[12,13]. However, these brittle materials suffer reliability issues for long-term use and have limited applications in flexible or wearable devices. Recently, there has been a growing interest in nanostructured piezoelectric semiconductors (for example, 1D wurtzite-structured nanowires and 2D atomically thin transition metal dichalcogenides (TMDCs)), because their low-dimensional geometries and superior mechanical properties facilitate their integration into flexible devices that can potentially sustain large strain. For example, ZnO nanowires can tolerate 5–7% strain without plastic deformation[14,15], and monolayer MoS_2 can sustain 11% in-plane strain[16]. More importantly, the long overlooked coupling between piezoelectric polarization and semiconductor properties in these materials gives rise to both novel fundamental phenomena and unprecedented device applications, which has led to increasing interest in the emerging fields of piezotronics and piezo-phototronics[17–24] (FIG. 1).

When polarization charges are induced in devices built from piezoelectric semiconductors, charge transport can be directly modulated by strain[24–28] (that is, the 'piezotronic effect'; BOX 1). The generation, separation, diffusion and recombination of photon-induced carriers can also be controlled by mechanical inputs[18,24,28–31] (that is, the 'piezo-phototronic effect'; BOX 2). These two effects provide new means of engineering interfacial properties and device operation without modifying the structure or chemistry of the interface, with a level of control that is not available using existing approaches. More detailed discussions on the fundamental principles of piezotronics and piezo-phototronics can be found in previous reviews[32,33]. Progress in these fields combined with emerging methods for deterministic production and the assembly of nanomaterials lead to

[1]*School of Materials Science and Engineering, Georgia Institute of Technology, Atlanta, Georgia 30332–0245, USA.*
[2]*School of Industrial Engineering, Purdue University, West Lafayette, Indiana 47907, USA.*
[3]*Beijing Institute of Nanoenergy and Nanosystems and National Center for Nanoscience and Technology (NCNST), Chinese Academy of Sciences, Beijing 100083, China.*

Correspondence to Z.L.W.
zlwang@gatech.edu

Article number: 16031
doi:10.1038/natrevmats.2016.31
Published online 10 May 2016

© 2016 Macmillan Publishers Limited. All rights reserved.

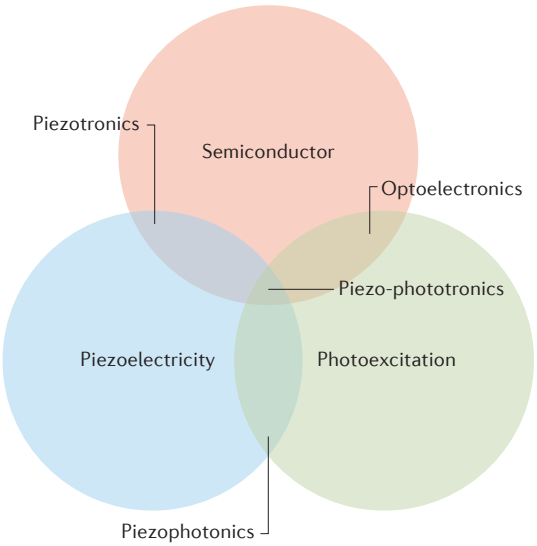

Figure 1 | **New research directions and applications of piezotronics and piezo-phototronics.** Coupling among piezoelectric, optical and semiconducting properties in piezoelectric semiconductor materials is the basis of piezotronics (piezoelectricity–semiconductor coupling), piezophotonics (piezoelectricity–photoexcitation coupling) and piezo-phototronics (piezoelectricity–semiconductor–photoexcitation coupling).

exciting research opportunities, from basic studies of piezoelectricity and semiconductor properties in functional nanomaterials to the development of 'smarter' electronics and optoelectronics. In this Review, we discuss recent advances in piezotronics and piezo-phototronics, and provide future perspectives for these emerging research areas.

Piezotronics

Understanding interfacial phenomena and interfacial engineering in semiconductor devices[34] is important for their application, for example, in electronics[35–37], optoelectronics[8,9,38,39] and catalysis[40,41]. In these fields, discontinuity in the local band structure and the resultant band alignment define the device characteristics. Although the band structure and alignment can be modulated by tailoring the interfacial properties (such as electronic transport) through external stimuli, this remains a relatively unexplored area for semiconductor nanodevices.

Piezotronics in 1D nanomaterials

1D piezotronics for adaptive electronics. Piezotronic devices are based on piezoelectric polarization as the 'gate' controlling signal, which is a fundamentally different mode of operation to conventional, electrically gated electronics. Since its inception in 2007, many experimental studies have revealed the fundamental nature of the piezotronic processes and implemented new device concepts. 1D ZnO nanostructures (for example, nanowires and nanobelts) have been the material of choice in most studies, because ZnO is a multifunctional material that holds great promise for applications in areas such as nanoelectronics, optoelectronics, sensors, photocatalysis and energy harvesting[42,43]. Moreover, compared with other piezoelectric semiconductors, it is relatively easy to synthesize ZnO nanostructures with controllable properties and desired morphologies through low-temperature approaches, such as hydrothermal solution processes[44,45]. Early examples of ZnO-based piezotronic devices include a strain-gated electromechanical switch and diode based on vertically and horizontally aligned ZnO nanowires[25,46,47]. Strain-induced polarization charges are also capable of modulating channel conductivity in such devices[48–52].

Following these early demonstrations, more complex piezotronic devices have been developed. By replacing the external gating voltage with piezoelectric polarization, two-terminal, strain-gated piezotronic transistors have been developed[17,26,53–55], in which the mechanical input asymmetrically modulates the band alignments at the two Schottky interfaces between the semiconductor and the electrodes, and acts as the gate signal for the device. It should be noted that mechanical strain also leads to changes in the band structure in semiconductors (that is, the 'piezoresistive effect'); however, the asymmetric change in the current–voltage curves observed for piezotronic transistors is characteristic of the piezotronic effect and cannot be caused by the nonpolar piezoresistive effect. Decoupling of the piezoresistive and piezotronic effects in the same piezoelectric semiconductor has been achieved in ZnO nanowires, in which the piezotronic effect dominates the strain-induced change in transport characteristics[56]. Piezotronic logic devices can be developed by integrating these strain-gated transistors to perform logic computations for the information carried by the mechanical stimulus[26,55]. A piezotronic resistive-switching nanodevice has also been demonstrated that can record the information encoded in the strain[57]. The feasibility of antimony-doped, p-type ZnO nanowires for piezotronics has also been investigated[58]. These experimental studies further demonstrated that piezoelectric polarization can effectively modulate the electronic transport in ZnO nanodevices. More importantly, the piezotronic principle offers a new approach for 3D structuring and integration of nanodevices[17] (FIG. 2). For example, it has been applied to design an independently addressable, two-terminal transistor array that allowed, for the first time, direct control of large-scale functional electronics by mechanical stimulation[17].

Many research groups have further demonstrated the existence of the piezotronic effect in other 1D piezoelectric semiconductors that are usually in the wurtzite phase (for example, GaN nanobelts and nanowires[59–61], CdS nanowires[62], CdSe nanowires[54,63], InAs nanowires[64] and InN nanorods[65]). Semiconductor materials of other crystal structures (for example, $ZnSnO_3$ nanowires with a rhombohedral structure[66,67] and CdTe nanowires in the zinc-blende phase[68]) have also been shown to exhibit piezoelectric properties. Moreover, alloyed structures containing a wurtzite semiconductor were observed to exhibit an enhanced piezotronic effect owing to the

© 2016 Macmillan Publishers Limited. All rights reserved.

Box 1 | **The piezotronic effect**

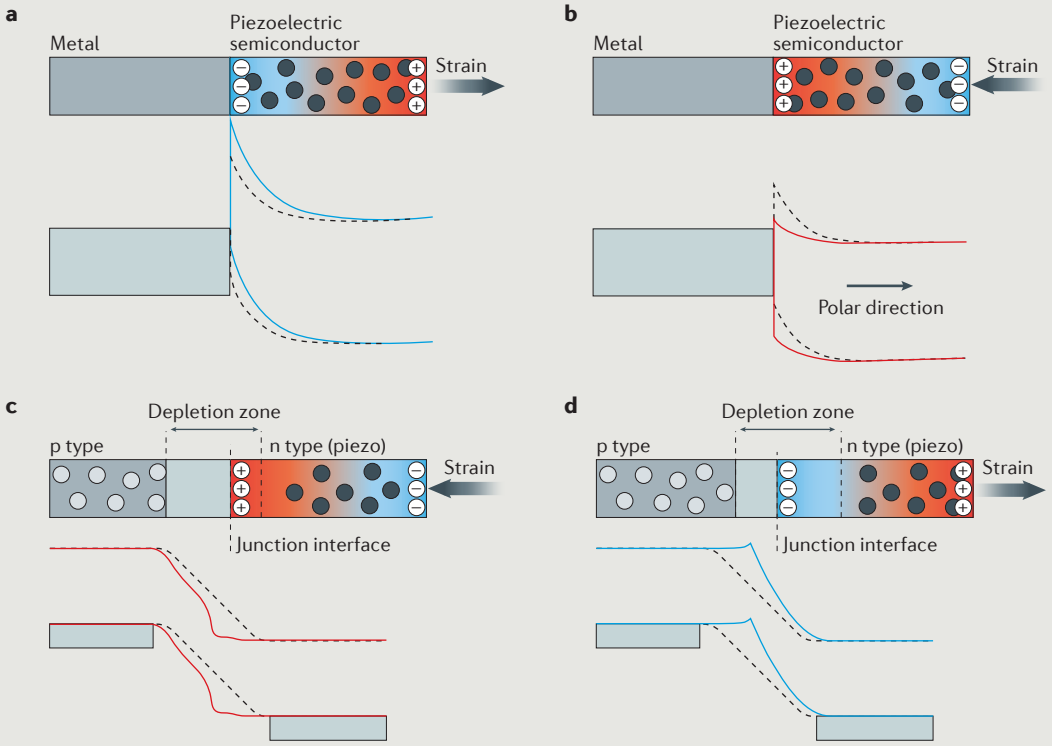

Owing to the direct piezoelectric effect and to the incomplete screening of polarization by free charges, a piezoelectric semiconductor upon straining can produce remnant polarization at its surface or at the interface with other materials[27,33]. This results in a redistribution of free charge carriers and alters the band structures near the interface through Coulombic interactions, allowing the modulation of electronic transport across the interface using dynamic mechanical inputs[24,33,195]. This coupling between piezoelectricity and electronic transport in piezoelectric semiconductors is referred to as the piezotronic effect[33,113,195].

An abrupt discontinuity in energy levels at the interface — the Schottky barrier — exists between metal electrodes and piezoelectric semiconductors[196]. Remnant piezoelectric polarization at the semiconductor side can significantly influence the Schottky barrier height (SBH) and other characteristics of the barrier. Upon straining of the semiconductor, the barrier interface is depleted of major carriers (for example, electrons for n-ZnO) with increased local SBH by the negative piezoelectric polarization (panel **a**); alternatively, the barrier interface can become less depleted by the positive piezoelectric polarization charges, resulting in a decreased SBH[24] (panel **b**). Therefore, strain-induced polarization can effectively modulate the electronic transport across the metal–semiconductor contact[28,197]. Other factors are also important; for example, the screening of piezoelectric polarization is an integral part of piezotronic coupling, which can be tuned by engineering the internal carrier concentration[57,58,74,76,198–202]. The work function of the contacting electrode is the other integral part of Schottky barrier-based piezotronic devices. Initial band bending at the Schottky contact in piezotronic devices not only depends on the chemical and structural conditions of the semiconductor surface, but also on the electrode materials and the interaction between the contacting materials[203].

If a p–n junction incorporates a piezoelectric semiconductor, the depletion region can enhance the electrostatic effect of the piezoelectric polarization owing to the diminished screening by residual free carriers[24] (panels **c** and **d**). For simplicity, only the band diagrams for a homojunction structure with an n-type piezoelectric semiconductor are depicted. When strain is introduced, the remnant piezoelectric polarization at the n-semiconductor side can affect the width and shape of the depletion layer and the local band alignment at the junction, effectively modulating the redistribution of charge carriers and hence the electronic transport in the junction. If positive polarization charges are induced on the n-type side, the depletion width on the p- and n-type sides increases and decreases, respectively, which expands and shifts the depletion region towards the p-type side (panel **c**)[170]. If the depletion layer on the n-type side further shrinks to the width of the piezoelectric polarization region, positive polarization charges may cause a downward band bending in the local band structure by electrostatically interacting with carriers in adjacent regions (panel **c**)[24,33]. This local deformation of the band structure creates a charge channel for trapping electrons. By contrast, if negative polarization charges are induced in the n-type region at the interface, the depletion width on the p-type side decreases and the depletion region is expanded and shifted towards the n-type side (panel **d**)[170]. A further increase in the applied strain causes an upward bend in the local band profile (panel **d**)[24,33]. Analogous effects are observed for more complex situations involving p–n heterojunctions or cases in which the p-type semiconductor is also piezoelectric[204]. Theoretical support for the band diagrams can be found in the literature[113,114,170,204].

© 2016 Macmillan Publishers Limited. All rights reserved.

Box 2 | **The piezo-phototronic effect**

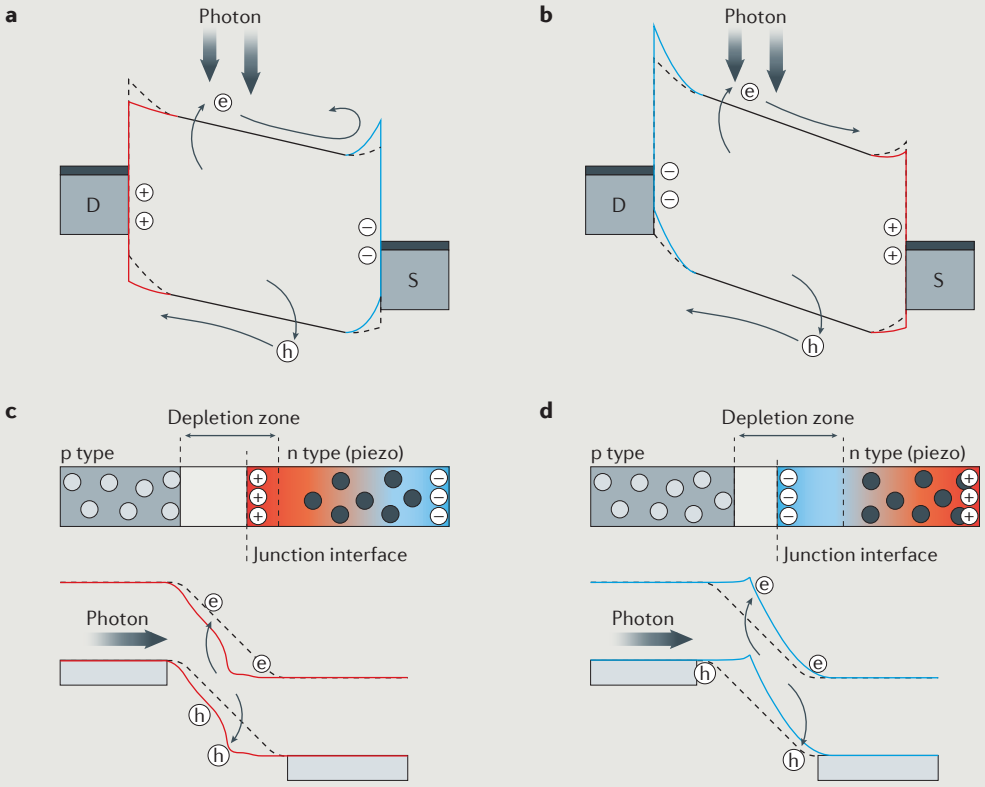

Interfacial strain-induced polarization can effectively modulate optical processes, such as the generation, separation, diffusion and recombination of charge carriers in optoelectronic devices built from piezoelectric semiconductors. This coupling among piezoelectricity, semiconductor properties and optical processes is referred to as the piezo-phototronic effect[24,33]. To describe this effect, a Schottky-contacted photodetector is used as an example of a device that typically involves the generation, separation and transport of photogenerated carriers[126]. The same argument can be applied to other optoelectronic devices. Incident photons induce electron–hole pairs in the piezoelectric semiconductor. Without applied strain, the electrons and holes are separated and collected by the built-in electric field at the Schottky contact. This gives rise to a photocurrent, which relies on the effective separation and transport of both types of carriers, and is strongly influenced by the barrier characteristics. When strain is introduced into the semiconductor, if positive polarization charges are created at the reversely biased Schottky contact, the realigned band profile provides a smaller driving force for the separation and redistribution of holes and electrons. Moreover, the energy barrier for electron transport at the positively biased contact is also increased. Therefore, the overall collection of photoinduced carriers in the device is suppressed (panel **a**). If negative polarization charges are created at the reversely biased Schottky contact, the band structure promotes the separation, transport and collection of holes and electrons (panel **b**). However, when the density of induced negative polarization charges at the reversely biased Schottky contact is large enough, strong upward bending of the valence band edge can create a new energy barrier for hole transport. Consequently, holes are trapped at the interface, which hinders the separation of photoexcited electron–hole pairs[126]. The related upward bending of the conduction band can lead to an increased dark current through enhanced tunnelling events, which deteriorates the overall photodetector performance. Thus, piezo-phototronic coupling is affected by the material properties of the device, such as the carrier concentration in the semiconductor and the work functions of the metal electrodes.

The photoresponse of a p–n junction results from the photogeneration of electron–hole pairs through band-to-band optical absorption[126]. The photogenerated electrons and holes are transported from the depletion layer by the built-in electrical field towards the n- and p-type regions, respectively, thereby creating a photocurrent. The band diagrams from BOX 1 are modified here to depict the piezo-phototronic effect (panels **c** and **d**). When positive piezoelectric polarization charges are induced in the n-type region (panel **c**), the expansion and shift of the depletion region towards the p-type side increases the effective series resistance for charge injection to the contact and hence decreases the device current. Meanwhile, the formation of a charge channel in the conduction band and the corresponding downward bending of the valence band edge on the n-type side result in less-effective separation of the electron–hole pairs[170]. By contrast, if negative polarization charges are induced at the junction in the n-type region, the expansion and shift of the depletion region towards the n-type side decreases the effective series resistance for charge injection to the contact and hence increases the device current (panel **d**). Moreover, the corresponding upward band bending can suppress electron–hole recombination and allow effective separation of the photogenerated carriers.

© 2016 Macmillan Publishers Limited. All rights reserved.

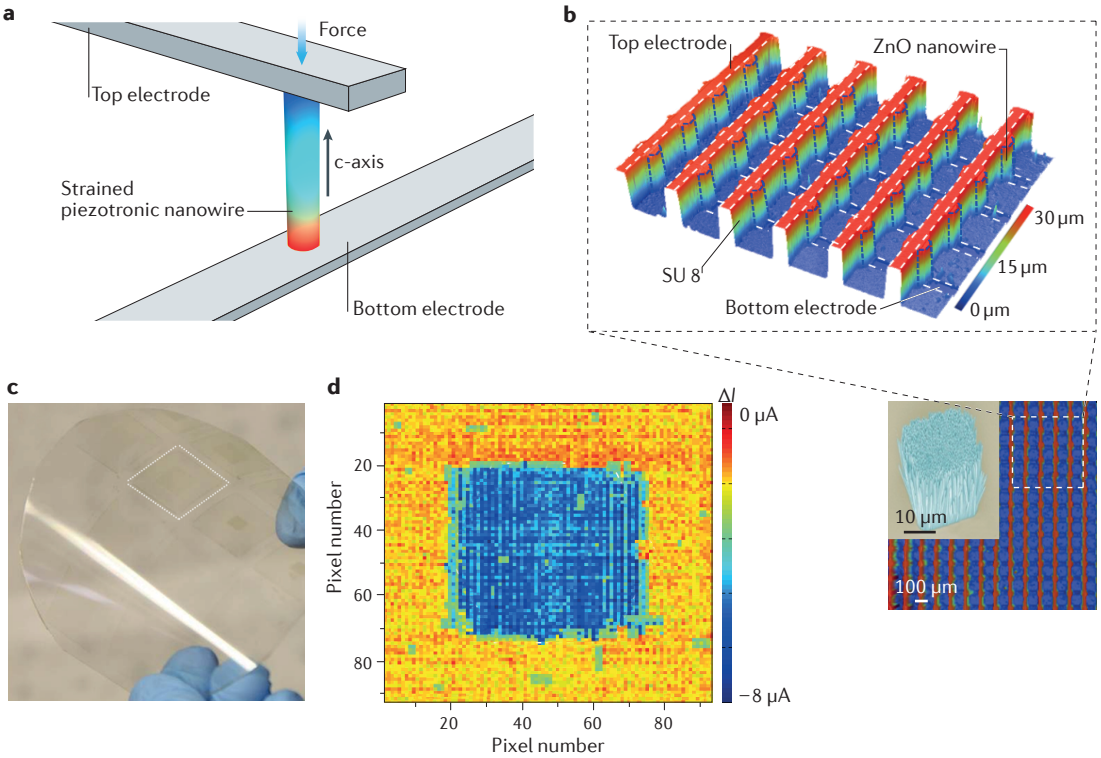

Figure 2 | **Array integration of vertical-nanowire piezotronic transistors for pressure imaging. a** | Schematic representation of a two-terminal strain-gated vertical piezotronic transistor. **b** | Device structure of a piezotronic transistor array and a scanning electron microscopy image of an individual pixel in the transister array. **c** | Photograph of a piezotronic transistor array on a flexible substrate. **d** | Electrical response from a piezotronic transistor array for imaging the spatial distribution of applied stress. Figure is reproduced with permission from REF. 17, AAAS.

enhancement of the piezoelectric constant through the alloying process and the suppressed screening of piezoelectric polarization[69,70]. In all of the studies above, a Schottky-contacted structure was used because of its simplicity in device design and fabrication. A thin insulator layer can also be integrated between the piezoelectric semiconductor and the electrode, forming a metal–insulator–semiconductor structure, in which the insulator layer reduces the carrier injection from the metal to the semiconductor. Consequently, screening of the piezoelectric polarization at the barrier interface is reduced and the piezotronic coupling can be substantially enhanced[71–73]. Piezotronics based on p–n junction devices have also been demonstrated when one or two of the semiconductors are piezoelectric[18,74]. Although recent advances in reliably producing p-type ZnO nanomaterials make it possible to implement a homojunction piezotronic device[74], most studies on p–n junction-based piezoelectric devices focus on the heterojunction structures formed between n-type ZnO and other p-type semiconductors[75–78].

It is noteworthy that in most of the reported piezotronics studies, the polarization field is directed along the conducting channel when the nanowire is axially strained, because many 1D piezoelectric semiconductors spontaneously grow along the polar direction. When subjected to transverse strain, polarization in these materials is perpendicular to the polar axis and can directly modulate the conducting channel. A recent theoretical study suggests that such a transverse configuration may be advantageous for mechanical sensing, because it avoids the buckling that is associated with axial compression[79]. The piezotronic effect in such materials has been recently characterized using *in situ* electron microscopy[22,80]. Some piezoelectric semiconductors can grow along the nonpolar directions, for example, *m*-plane GaN nanowires[81], *a*-axis GaN nanobelts[82,83] and ZnO nanobelts[84]. These examples provide a unique material platform for understanding the fundamental coupling between piezoelectric polarization and the charge carriers in the conducting channel, as well as for guiding the design and development of future piezotronic devices.

Nanosensors enhanced by the piezotronic effect. The stimulus-responsive change of the Schottky barrier height (SBH) is the basis of Schottky-contacted sensors[85]. In devices incorporating piezoelectric semiconductors, strain-induced polarization can modulate the SBH and thus control the interfacial energy levels at the contact; this can significantly enhance the performance of Schottky barrier-based nanosensors[72,86–92]. Early demonstrations include ZnO nanowire sensors with improved performance for detecting biomolecules (for example, protein and glucose[89,91]), pH levels[90] and gas species (for example, oxygen[92]) under the application of external strains. Based on the same principle, recent progress has been made in developing sensitive

© 2016 Macmillan Publishers Limited. All rights reserved.

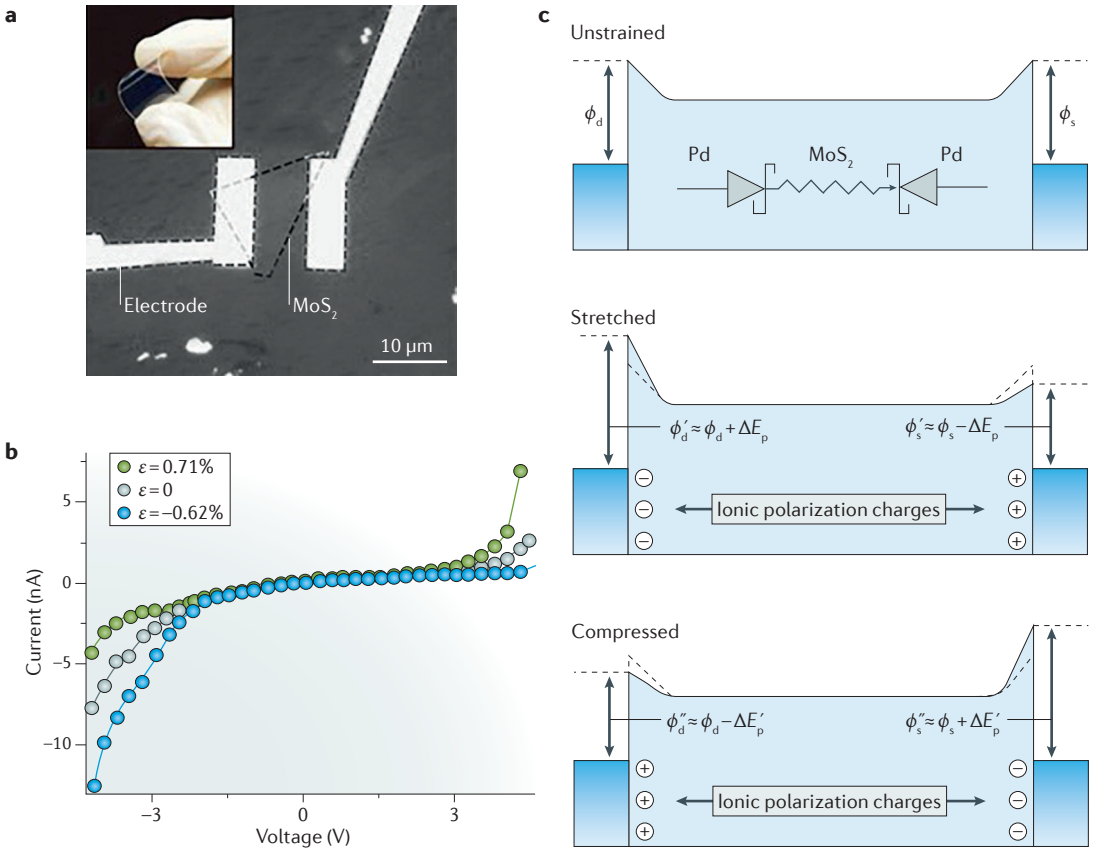

Figure 3 | **Piezotronics in atomically thin piezoelectric semiconductors. a** | A flexible piezotronic device based on monolayer MoS_2. **b** | The piezotronic response in the monolayer MoS_2 device shown in panel **a** under application of static uniaxial strain. **c** | Band diagrams depicting the piezotronic behaviour observed in panel **b**. ϕ_d and ϕ_s, Schottky barrier heights formed at the drain and source contacts, respectively; ε, strain; E_p, change in the Schottky barrier height by piezoelectric polarization charges. Figure is from REF. 19, Nature Publishing Group.

and responsive nanosensors by integrating piezoelectric semiconductors and Schottky interfaces on flexible substrates. For example, ZnO nanowire sensors under compressive strain possess superior performance compared with their strain-free states, in terms of sensitivity and sensing resolution, for detecting trace amounts of hydrogen peroxide released from biological cells[87]. The piezotronic effect in ZnO nanowires can also promote and enhance drug metabolism and detection in the presence of human cytochrome P450 enzymes, which are critical for the metabolism of many endogenous and exogenous compounds found in therapeutically important drugs[93]. When a small static compressive strain was applied, the sensitivity of the device to the drug was improved by more than 420%. A similar principle was applied to improve the performance of a ZnO nanowire sensor for the detection of flammable (for example, hydrogen) and toxic (for example, nitrogen dioxide) gases at room temperature, for which the detection sensitivity was improved by 5359% for hydrogen and 238.8% for nitrogen dioxide sensing when uniaxial strains were applied[94]. The performance of ZnO nanowires as humidity sensors can also be enhanced by the piezotronic effect[95]. It is expected that this principle can be extended to other sensing applications.

Piezotronics in 2D piezoelectric semiconductors

Monolayer MoS_2, $MoSe_2$ and other TMDCs are theoretically predicted to exhibit piezoelectricity owing to the absence of inversion symmetry in their crystal structures[96–98]. This, combined with their high crystallinity, outstanding semiconducting properties (for example, a bandgap of ~1–2 eV and room temperature mobility >200 $cm^2\ V^{-1}\ s^{-1}$)[6,99] and superior mechanical properties (for example, a monolayer MoS_2 crystal has a higher Young's modulus than steel and can be deformed by 11% without fracture)[16,100], makes 2D TMDCs promising high-performance electromechanical materials for piezotronic devices. Recently, the first experimental observation of piezoelectricity in mechanically exfoliated monolayer MoS_2 was reported[19] (FIG. 3a–c). For this atomically thin piezoelectric semiconductor, it was shown that strain-induced polarization can modulate charge-carrier transport at the Schottky barrier[19]. Strain can also induce changes in the band structure of MoS_2 through the piezoresistive effect[101]. The anisotropic changes in the current–strain curves shown in FIG. 3b are not caused by the piezoresistive effect, but from the modulation of the SBH at the reversely biased metal/MoS_2 barrier by polarization charges induced at the zigzag edges of MoS_2

© 2016 Macmillan Publishers Limited. All rights reserved.

(REF. 19). The piezoelectric measurements in FIG. 3b were also used to determine the crystallographic orientation of the MoS_2 flakes. A layer dependence in piezoelectricity and the piezotronic effect in atomically thin MoS_2 was observed, in which monolayer MoS_2 had a strong piezotronic response, whereas bilayer and bulk flakes had a pure piezoresistive response[19,102]. This dependence, which is attributed to the recovery and breaking of centrosymmetry in MoS_2 flakes with even and odd numbers of layers, has never been reported for any other material. Phenomena such as this provide new knowledge in structure–property–performance relationships in atomically thin materials and may enable unprecedented engineering capability in designing and processing novel functional materials.

Compared with exfoliation methods to grow MoS_2, chemical vapour deposition (CVD) is more technologically appealing because it allows large-scale production. Moreover, the naturally formed triangular morphology in CVD-grown MoS_2 allows easy identification of its crystal orientation, which is important for piezotronic studies[103]. Recently, the piezoelectric effect and strain-dependent conductivity changes were observed in monolayer CVD-grown MoS_2 (REF. 20). It was later shown that exfoliated monolayer MoS_2 exhibits a piezoelectric coefficient comparable to wurtzite-structured materials, such as ZnO (REF. 104); however, the effect of piezoelectricity on electronic transport was not investigated. The piezoelectricity and large mechanical flexibility of monolayer MoS_2 shown in these very few early studies demonstrate the potential

Table 1 | **Main theoretical models and simulation methods used in piezotronics and piezo-phototronics**

Theoretical model	Simulation method	Major assumptions	Conclusions
Piezotronics			
Semi-analytical abrupt junction model that integrates the governing equations for semiconductor physics and piezoelectricity[113,114]	Analytical calculations and FEM	• Material dimensions are large • Abrupt depletion layer • Non-degenerate semiconductor • Low injection • Piezoelectric charges distribute at the interface within a finite width	The effect of piezoelectric charges on charge-carrier transport is considered as a perturbation: $J = J_0 \exp\left(\frac{qe_{33}s_{33}W_{piezo}}{2\varepsilon_s kT}\right)\left[\exp\left(\frac{qV}{kT}\right)-1\right]$ where e_{33} is the piezoelectric constant, s_{33} is the strain along the polar axis, W_{piezo} is the width within which piezoelectric charges distribute.
Atomic structure model of a metal–ZnO–metal piezotronic transistor[116]	*Ab initio* DFT	• The Ag (111) plane directly contacts the polar planes of ZnO • The in-plane lattice constants of the transistor supercell are chosen to match those of bulk ZnO	Modulation of the SBH is asymmetric at the two contacts. Transport of the strain-dependent carriers mainly depends on W_{piezo}, the piezoelectric semiconductor materials and the electrode metal used. This provides quantitative information relating to W_{piezo}.
Quantum scattering model in the ballistic regime[117]	Quantum scattering theory-based numerical calculation	• The piezopotential is treated as a potential barrier at the interfaces • The piezotronic device is in the ballistic regime	The threshold gate voltage is influenced by the piezoelectric effect. The electrical current fluctuates when the gate voltage is in the threshold region owing to quantum tunnelling resonance.
Size-dependent electromechanical model[121]	FEM	The size-dependent mechanical properties affect the piezoelectric charges through coupling with the size effects in electronic transport.	Mechanical and electrical properties in piezoelectric semiconductor nanostructures can cause interference in piezotronic applications.
Monolayer semiconductor model[125]	DFT	• The Pd atoms in the inner electrode are considered as fixed • The zigzag edges of MoS_2 are in direct contact with the Pd (111) plane • The lattice mismatch between Pd and MoS_2 is ignored	The metal/MoS_2 interface enhances the piezotronic effect by breaking metallic-state screening at the MoS_2 edge.
Piezo-phototronics			
1D semi-analytical model that integrates the governing equations for piezoelectricity, optical, and electronic processes in piezoelectric semiconductors[127,128,169]	Analytical calculations and FEM	• Material dimensions are large • Abrupt depletion layer • Non-degenerate semiconductor • Piezoelectric charges distribute at the interface within a finite width	Strain-induced polarization charges can effectively modulate the generation, separation, transport and recombination of photoinduced carriers by modifying the band structure.
2D FEM model that takes into consideration the device geometry[170]	FEM	• Material dimensions are large • Abrupt depletion layer • Piezoelectric charges distribute at the interface within a finite width	• Piezoelectric charges can result in the shift of the depletion region and the formation of a charge channel at the interface • Lower nanomaterial doping and smaller nanomaterial size are favourable • A homojunction structure is potentially more favourable than a heterojunction structure

DFT, density functional theory; FEM, finite-element method; SBH, Schottky barrier height.

© 2016 Macmillan Publishers Limited. All rights reserved.

for applications in novel electromechanical devices. Inspired by these experimental works, there has been rapid progress in the theoretical study of piezoelectricity in a broad range of 2D materials[105–108]. Studies have revealed that, in addition to TMDCs, other 2D compounds are piezoelectric, such as monolayer group IV monochalcogenides (SnSe, GeS and SnS)[105,106], group III monochalcogenides (GaSe, GaS and InSe)[107] and transition metal dioxides (SnO_2, HfO_2 and MoO_2)[108]. The study of the fundamental piezotronic effect in 2D atomically thin crystals could lead to the development of piezotronic applications based on these materials.

Piezotronics in semiconducting thin films

The piezotronic effect is pervasive and does not just occur in nanostructured single-crystalline materials. Considering that the success of semiconductor technology is enabled by thin-film processes, exploiting the piezotronic effect in thin-film devices could be a way of overcoming some of the limitations of nanomaterials: for example, the difficulty in large-scale production, non-uniformity and reliability. In the first attempt to study the piezotronic effect in thin-film materials[109] in 2013, the alignment of the polar axes in sputtered ZnO columnar grains resulted in piezoelectricity and piezotronic coupling in the polycrystalline thin film. Recently, the piezotronic effect in a ZnO nanowire film and its application in temperature sensing was also investigated[110]. In a different configuration, the effect of uniaxial stress on the electrical properties of a commercial ZnO varistor ceramic was studied[111]; it was found that the current response of the varistor possessed a strong stress dependence. Such behaviour can be explained with a modified piezotronic theory, in which changes in the electrostatic barrier at grain boundaries are caused by induced piezoelectric charges that depend on the relative orientation of the polarization in adjacent grains. Moreover, increasing the uniaxial stress was shown to lead to a higher current through a polycrystalline ZnO varistor, which can be attributed to the lowering of the SBH at the grain boundaries via the piezotronic effect[23]. Finally, it was recently shown for the first time that the piezotronic effect can either enhance or diminish the natural asymmetry of the *I*–*V* characteristics in double Schottky barriers — the symmetric potential barriers formed by trapped electrons at grain boundaries in polycrystalline semiconductors — depending on the stress direction and the relative polarization orientations of adjacent grains[112].

Advances in the theory of piezotronics

The basic governing equations of piezoelectricity and semiconductor physics can be integrated to semi-analytically describe the coupling between piezoelectric polarization and electronic charges in piezotronic devices. Specifically, the band profiles and charge transport can be expressed as functions of piezoelectric polarization and applied strain. The changes in energy band profiles and electronic transport in piezotronic devices have been analytically derived under static strain by considering strain-induced polarization as a small perturbation to the band structure at the interface within the well-established semiconductor device theory[113]. For example, the potential distribution, $\varphi_i(\chi)$, which is directly related to the energy of the band edge in the device inside a strained p–n junction, can be expressed as follows when only the n-type material is piezoelectric[113],

$$\varphi_i(\chi) = \begin{cases} \dfrac{qN_A\,(x+W_{Dp})^2}{2\varepsilon_s}, & -W_{Dp} \le x \le 0 \quad (1) \\ \varphi_i(0) + \dfrac{q}{\varepsilon_s}\left[N_D\left(W_{Dn} - \dfrac{x}{2}\right)x + \rho_{piezo}\left(W_{piezo} - \dfrac{x}{2}\right)x\right], & 0 \le x \le W_{piezo} \quad (2) \\ \varphi_i\,(W_{piezo}) - \dfrac{qN_D}{\varepsilon_s}\left(W_{Dn} - \dfrac{W_{piezo}}{2}\right)W_{piezo} + \dfrac{qN_D}{\varepsilon_s}\left(W_{Dn} - \dfrac{x}{2}\right)x, & W_{piezo} \le x \le W_{Dn} \quad (3) \end{cases}$$

where q is the electronic charge, $N_A(x)$ and $N_D(x)$ are the acceptor and donor concentrations, respectively, W_{Dn} and W_{Dp} are the depletion widths on the n and p side, respectively, ε_s is the permittivity of the material, $\rho_{piezo}(x)$ is the density of the piezoelectric polarization charges (in units of electron charge), and W_{piezo} is the width of the layer within which the piezoelectric charges are distributed.

The existence of piezoelectric polarization charges give rise to the shift in band edge, as illustrated in BOX 1. At a p–n junction or Schottky contact, carrier transport can be effectively controlled by the applied strain (see TABLE 1 for an overview of the different models used and the conclusions drawn from them). Numerical simulations have been used to verify the analytical models and to predict the properties of piezotronic devices. For example, the numerical results presented in two papers[113,114] confirmed the shift in band edge and the deformation in Schottky contacts and p–n junctions under strain. These results have led to a more qualitative interpretation of experimental findings and provided guidance for the subsequent design of piezotronic materials and devices. However, the semiclassical approach adopted in these studies falls short of providing the desired level of insight into the underlying mechanism. For example, the distribution of piezoelectric charges in the semiconductor — an important factor that affects piezotronic coupling — is assumed to be confined to within a few atomic layers[113]; such information cannot be provided by or be incorporated into the classical approach. Furthermore, classical piezotronic theory may only be satisfactory when the dimensions of the device are relatively large (for example, much larger than the de Broglie wavelength of an electron)[115] but could collapse when quantum effects can no longer be ignored.

Recent progress has been made in addressing these issues using various advanced approaches. In one example, an *ab initio* computational study of the piezotronic effect was conducted using the atomic and molecular structure based entirely on quantum mechanics and basic physical constants[116]. It was concluded that modulation

© 2016 Macmillan Publishers Limited. All rights reserved.

of the local contact via the piezotronic effect depends on the magnitude and polarity of the applied strain, as well as the intrinsic properties of the materials that form the interface (for example, the carrier density and charge screening lengths). Quantitative information about the width of the piezoelectric charge distribution at the interface was also revealed, which provided the first quantum mechanical understanding of the piezotronic effect and established its physical basis. In another study[117], electron transport was treated as a quantum wave on the basis of quantum scattering theory, and the transmission coefficient of the electrons in the ballistic regime was calculated accordingly. This study suggested that the threshold gate voltage of the quantum piezotronic transistor is influenced by the piezoelectric effect, and that the electrical current fluctuates when the gate voltage reaches a threshold owing to quantum tunnelling resonance. These results not only provide a more profound understanding of the electrostatic coupling between the piezoelectric polarization and the electrons, but also help shed light on the design and implementation of next-generation quantum piezotronic devices (for example, piezotronic tunnel junctions[118–120]).

Prior work on modelling piezotronic devices has seldom addressed the size-dependent, electrical–mechanical coupling effect. The piezotronic process has only been studied assuming a constant elastic modulus for the semiconductor, without considering the size-dependent mechanical properties. By modelling the strengthening effect using the finite-element method, mechanical and electrical properties in piezoelectric semiconductor nanostructures were suggested to interfere for piezotronic applications[121]; this study provided guidelines for designing high-performance piezotronic nanodevices with proper scaling. Moreover, the thermal effect in nanowires can strongly affect piezotronic coupling, because the pyroelectric effect introduces additional volume and surface charges at the boundaries[122]. The nonlinear behaviour of piezotronic transistors has also been recently investigated, which might be of interest for the development of nonlinear piezotronic circuits[123]. In addition to the progress made in modelling ZnO-based piezotronics, recent theoretical studies revealed that the piezotronic effect can be enhanced by incorporating core–shell wurtzite III–V semiconductor structures[124] or by adopting tubular nanostructures[59]. Inspired by the recent experimental observation of the piezotronic effect in single-atomic-layer MoS_2 (REF. 19), the first theoretical study was recently carried out for a single-layer MoS_2 piezotronic transistor using density functional theory[125]. It was concluded that the metal/MoS_2 interface has an essential role in enhancing the piezotronic effect by breaking the metallic state screening at the MoS_2 edge. Collectively, these theoretical studies have led to a deeper understanding of the underlying mechanisms related to the piezotronic effect.

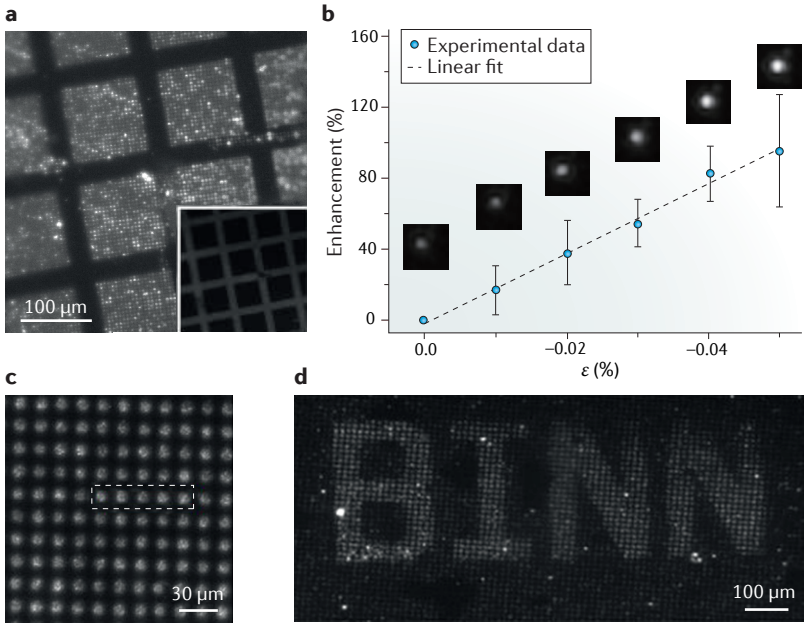

Figure 4 | **Piezo-phototronic LED array for pressure imaging. a** | Optical image of a light-emitting diode (LED) array formed by a ZnO-nanofilm/Si-micropillar heterostructure. **b** | Enhancement in light emission under different strains. **c** | Optical images of a ZnO-nanowire/p-polymer LED array. **d** | Electroluminescence image of the device under a stress of 80 MPa. ε, strain. Panels **a** and **b** are reproduced with permission from REF. 154, Wiley-VCH. Panels **c** and **d** are reproduced with permission from REF. 156, Wiley-VCH.

Piezo-phototronics

Dynamic manipulation of electronic and optical processes in optoelectronics is usually achieved by applying an electrostatic bias[126]. However, emerging applications, such as wearable and human–machine-interfacing devices, require functional optoelectronics to be directly regulated by mechanical inputs from their environment. The local band structure and resultant band alignment can be effectively modulated by strain-induced polarization. The coupling among piezoelectricity, semiconductor charge transport and optical processes in piezoelectric semiconductors provides a new mechanism — the piezo-phototronic effect — to modulate the behaviour of photoexcited carriers and engineer new optoelectronic devices[127–129]. The basic principle of the piezo-phototronic effect is described in BOX 2.

Piezo-phototronics for active optoelectronics

Optoelectronic devices that use strain-induced interfacial polarization as the controlling signal — piezo-phototronics — are fundamentally different from electrically controlled optoelectronic devices. After the first reports in 2010 on the coupling between piezoelectricity and photoexcitation in ZnO nanowires[24,130], experimental studies were performed for various devices, such as strain-gated flexible light-emitting diodes (LEDs), photodetectors and solar cells[18,29–31,78,128,129,131–137]. Photoelectrochemical processes can also be tuned by piezoelectric polarization at the semiconductor/electrolyte interface, leading to either an enhancement or reduction of the photocurrent when tensile or compressive strains are applied to the piezoelectric semiconductor anode[27,138,139]. Although the effect of strain on the optical properties of bent ZnO nanowires has been widely studied through probing the strain-induced changes in band structure[140–145], the piezo-phototronic effect of ZnO nanowires has not been considered until

© 2016 Macmillan Publishers Limited. All rights reserved.

recently. To reveal the microscopic origin of strain effects in ZnO nanowires, piezotronic modulation of the local spatial distribution of photoexcited carriers needs to be taken into account[146].

Piezo-phototronics in photodetectors. Photodetectors operate on the basis of the separation of photon-generated electron–hole pairs by either a p–n junction or a Schottky barrier. In Schottky-barrier-based photodetectors, the characteristics of the SBH determine the detector performance. For example, the photoresponse of a ZnO–Au ultraviolet (UV) detector can be enhanced through piezotronic engineering[147], which promotes the separation and extraction of the photoexcited carriers at the Schottky barrier. In this example, a 440% enhancement of photocurrent and a fivefold increase in sensitivity were achieved when a static strain was applied to the nanowire photodetector. Recently, a flexible GaN photoswitch with strain-enhanced photodetection was reported[148], which led to an enhancement of the UV detection on/off ratio of up to 154% at zero bias under the application of static strain. The reduced screening of piezoelectric polarization at the barrier owing to the metal–insulator–semiconductor structure can significantly enhance the piezotronic modulation of the photoexcited carriers[72,73]. Interestingly, when the applied strain exceeds a threshold, the dark current in the metal–insulator–semiconductor photodetector increases owing to increased tunnelling through the barrier[73], as depicted in the band diagrams in BOX 2.

Recently, progress has been made in improving the performance of p–n heterojunction photodetectors through the piezo-phototronic effect. An n-ZnO nanowire/p-NiO photodetector was shown to exhibit a strain-dependent photoresponse[149], and the photoresponse decay time in such a heterojunction device can be modulated using the piezo-phototronic effect[150].

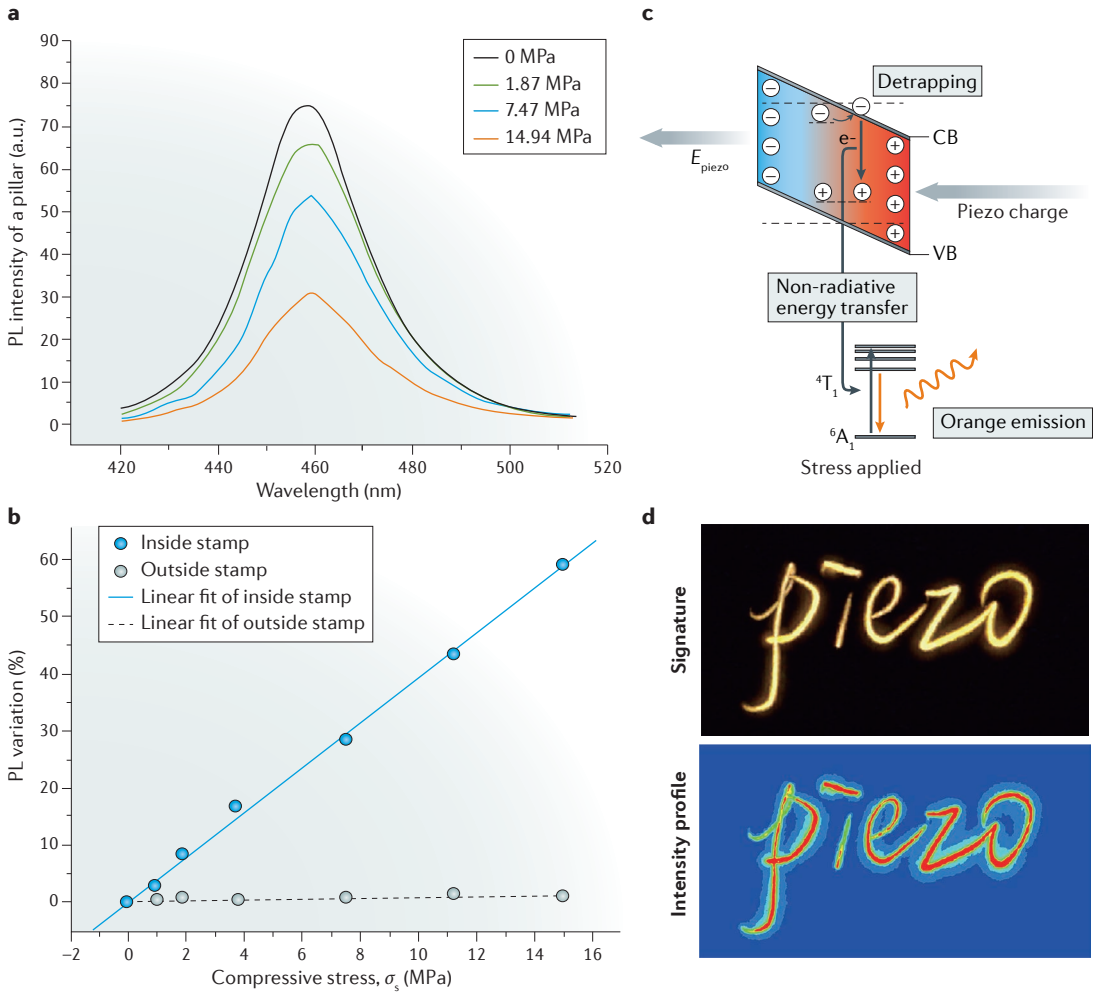

Figure 5 | **Piezo-phototronic luminescence devices for adaptive sensing. a** | Photoluminescence from a multi-quantum-well array under various stresses. **b** | Photoluminescence intensity as a function of compressive stress (σ_s). **c** | Mechanism of mechanoluminescence produced by the piezo-phototronic effect in certain materials (for example, a flexible sensor based on manganese-doped ZnS particles). **d** | Piezo-phototronic luminescence devices for recording the writing pattern and force applied during writing. a.u. arbitrary units; CB, conduction band; PL, photoluminescence; VB, valence band; E_{piezo}, the piezoelectric field. Panels **a** and **b** are reproduced with permission from REF. 160, American Chemical Society. Panels **c** and **d** are reproduced with permission from REF. 163, Wiley-VCH.

© 2016 Macmillan Publishers Limited. All rights reserved.

Similar processes have been reported in heterojunctions formed between n-ZnO nanowires and other semiconductors. For example, piezo-phototronic photosensing with an enhancement in sensitivity of over 700% was achieved in an optical fibre–nanowire hybrid structure[151], which consisted of a ZnO–CdS nanowire heterojunction that was synthesized coaxially around the optical fibre. Similarly, the performance of a type-II heterojunction photodetector based on a ZnO–ZnS core–shell nanowire was considerably improved, with an enhancement of three orders of magnitude in relative responsivity under a compressive load[152]. The piezo-phototronic coupling between polarization charges and photogenerated carriers can further modulate the optoelectronic process in silicon-based photodetectors, thus demonstrating the great potential of piezo-phototronic devices to be integrated with state-of-the-art semiconductor technology[69,153]. The performance of p-Si/ZnO photodetectors for visible light sensing can be optimized by tuning the transport of charge carriers across the Si/ZnO interface with piezoelectric polarization[153]. An enhancement of 177% in photoresponsivity and a reduction of 87% in response time were obtained when a compressive strain was introduced to the ZnO. The piezo-phototronic effect can be further enhanced by alloying the ZnO with other elements, for example, magnesium[69]. Both the photodetector performance and the piezo-phototronic effect increase with magnesium content owing to the enhanced piezoelectric coefficient that results from the alloying process. Piezo-phototronic modulation of photoexcited carriers has been further studied in other materials systems, for example, the CdSe–ZnTe core–shell structure, in which the piezoelectric effect in the CdSe core layer effectively controls the separation and transport of charge carriers at the CdSe/ZnTe interface[63].

Piezo-phototronics in light-emitting diodes. Light emission from semiconductors depends on the efficiency of carrier injection, recombination and extraction. Recently, an LED array based on a ZnO nanofilm/p-Si micropillar heterostructure was reported[154], the emission intensity of which could be enhanced by applying compressive strain (FIG. 4a,b); this was achieved through the effective modulation of the injection, transport and recombination of electron–hole pairs by the piezo-phototronic effect at the ZnO/Si interface. The same control and adaptive performance were demonstrated in organic–inorganic hybrid LEDs based on ZnO nanowires and p-type polymers[155]. The emission intensity of the hybrid LED array can be enhanced by applying compressive strain. Furthermore, a flexible LED array composed of p-type PEDOT:PSS and patterned ZnO nanowires was developed for mapping the spatial pressure distributions through the piezo-phototronic effect[156]. The emission intensity was determined by locally applied strains, which controlled the transport and recombination of electrons and holes in the individual LEDs. Therefore, the spatial distribution of the applied pressure can be obtained by parallel reading the emission intensities of the device (FIG. 4c,d).

Piezophotonic LEDs can also be used for visible light communication, as recently demonstrated for InGaN–GaN multi-quantum-well (MQW) nanopillars, in which the information was coded by mechanical straining and the output (that is, the photoluminescence intensity) was defined using binary logic for the real-time data transmission[157]. Polarization charges increase the internal electric field of the InGaN–GaN MQW active region and effectively tilt the band edges in the MQW structure, thereby reducing the overlap between the electron and hole wavefunctions in the quantum wells and thus decreasing the emission intensity from the LEDs when static compressive strain is applied. In addition to such vertical LED configurations, a horizontally aligned piezo-phototronic LED array has also been demonstrated using a ZnO/p-GaN structure[158]. The electroluminescence properties of the device can be controlled through piezoelectric polarization during assembly. The corresponding piezo-phototronic process results in a decrease in the intensity of the UV to blue emission accompanied by a redshift of the emission peak, disappearance of the 3.08-eV electroluminescence transition and an increase of the deep energy level related to yellow to green emission. These results demonstrate that the emission colours can be tuned in ZnO/p-GaN LEDs through the piezo-phototronic effect and highlight the potential of these devices in pressure transduction applications.

Piezo-phototronics in luminescence applications. All-optical systems have the potential to transfer digital information faster and with higher data capacity[159]. Recently, a dynamic pressure sensor array of InGaN–GaN MQW nanopillars was presented based on piezo-phototronically tuned photoluminescence imaging[160]. In this device, the photoluminescence intensity can be modulated linearly by the mechanical strain (FIG. 5a,b): when the nanopillars are subjected to strain, piezoelectric polarization induced at the quantum well interface can control the excitation and recombination processes. By measuring the photoluminescence signals from the nanopillar array, the pressure distribution can be mapped in real time[160]. Piezo-phototronic coupling in phosphors has also been studied. For example, mechanically tunable luminescence of manganese-doped ZnS grown on a piezoelectric lead magnesium niobate–lead titanate (PMN–PT) substrate was demonstated[161]. The light emission of the manganese-doped ZnS phosphor was induced by the piezoelectric field from the PMN–PT substrate, which represents a new type of coupling between piezoelectric and photonic processes. Following this work, the design was improved by mixing metal ion-doped ZnS in a transparent polymer to form flexible composite phosphors[162]. White light emission from the flexible luminescence device was observed when tensile strain was applied, with the intensity strongly depending on the applied strain rate.

Using a similar design, dynamic pressure mapping was achieved using a flexible sensor matrix that incorporated manganese-doped ZnS particles[163] (FIG. 5c,d). In this case, piezoelectric polarization charges induced in ZnS tilt the conduction and valance bands of ZnS,

© 2016 Macmillan Publishers Limited. All rights reserved.

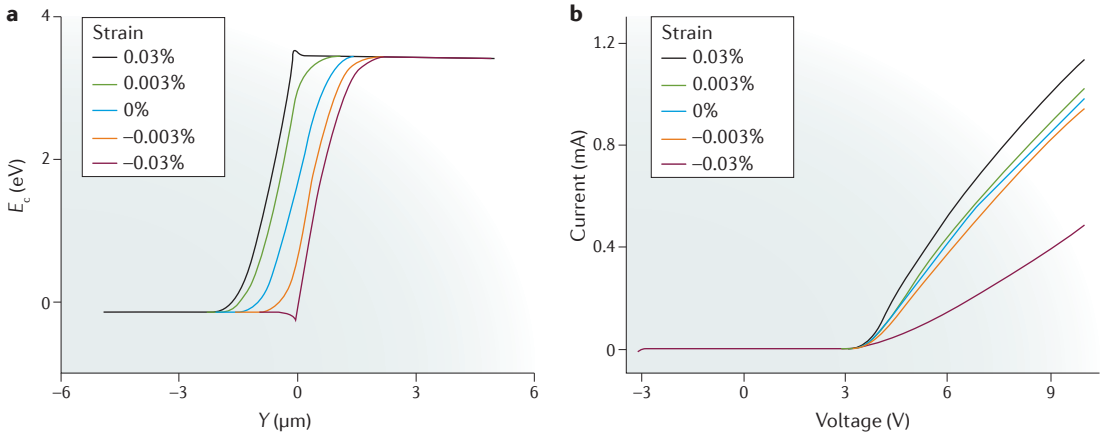

Figure 6 | **Numerical simulations of strain-induced band deformation and device operation in piezo-phototronics.** **a** | Conduction band deformation of an n-ZnO/p-type structure under different strains applied to the ZnO layer. **b** | Current–voltage characteristics of the strained piezo-phototronic device corresponding to the band structures in panel **a**. E_c, conduction band edge in ZnO; *Y*, location in the p–n junction. Figure is reproduced with permission from REF. 170, Wiley-VCH.

detrapping the bound electrons in impurities near the conduction band edge; these electrons can transit to holes in the valence band, resulting in the release of energy (FIG. 5c). The released energy excites the Mn^{2+} dopant ions, and photon emission occurs when the excited Mn^{2+} ions fall back to the ground state. Very recently, by coupling the magnetic field to the piezo-phototronic process, a magnetic-induced-luminescence device was developed from flexible composite laminates, which emitted green and white light[164]. The light emission could be modulated in a reversible and dynamic manner through strain-mediated coupling by controlling the weak magnetic field. Piezo-phototronic luminescence devices, such as those detailed above, offer new possibilities in energy harvesting, non-destructive sensing and stimuli-responsive multimodal bioimaging[165].

Piezo-phototronics in other applications. The piezo-phototronic principle can also be applied to other applications: for example, the development of highly efficient photoelectrochemical photoanodes[21]. It was recently demonstrated that the oxygen evolution reaction (OER) can be improved by engineering the interfacial band structure of a ZnO–$Ni(OH)_2$ heterojunction through the piezo-phototronic effect[21], whereby substantially enhanced photocurrent density from the oxidation reactions was obtained by physically deflecting the photoanode. In this example, polarization charges induced at the junction interface drive additional photoexcited carriers from ZnO towards the interface for the OER. This might provide a new route for improving the performance of inexpensive catalysts for solar fuel production. In a separate study, a hybrid photocatalyst was designed by assembling TiO_2 nanoparticles on piezoelectric ZnO nanoplatelets[166]. The photocatalysis process was enhanced by up to 20% by tuning the thermal stress in ZnO through the controlled cooling of the hybrid photocatalyst. The induced piezoelectric polarization charges could effectively separate the photogenerated charge carriers at the heterojunction interface between ZnO and TiO_2.

The piezo-phototronic effect has also been used in mechanical-electro-optical logic computations and information storage[167]. Strain-induced polarization charges at the electrode/CdS interface can gate the electrical transport and optoelectronic processes of charge carriers, such that the mechanical and optical stimuli can be processed to electronic signals through the piezo-phototronic effect. Such capabilities are not available in existing technologies and this therefore provides great versatility and the potential for developing adaptive electronics and optoelectronics, for example, for applications in human–machine-interfacing devices and optical nanoelectromechanical systems. Piezo-phototronic coupling in solar cells based on sputtered ZnO films and p-type polymers has also been investigated[168].

Theoretical studies of piezo-phototronics

Similar to the case for piezotronics, early theoretical studies of piezo-phototronics semi-analytically described coupling among piezoelectric polarization, optical processes and electronic transport[127,128,169] by incorporating terms for strain-induced polarization into classical semiconductor theory. Numerical simulations were then performed to describe the observed experimental results semi-quantitatively. However, these early theoretical works were limited to 1D models and did not take the device geometry into consideration. Moreover, it was assumed that the depletion region experiences negligible change in width under strain and that the induced piezoelectric charges only affect the local potential distribution[113]. These assumptions are valid when the carrier concentration in the piezoelectric semiconductor is large (~10^{17} cm^{-3}), such that the total number of depletion charges is larger than the number of piezoelectric polarization charges; this is the case for hydrothermally grown ZnO nanowires[170]. However, these assumptions

© 2016 Macmillan Publishers Limited. All rights reserved.

may not hold for low doping concentrations, such as those in ZnO nanowires grown from high-temperature vapour deposition (~10^{14}–10^{15} cm^{-3})[170].

A method for 2D simulation of the piezo-phototronic effect in a p–n junction was recently developed[170]. The finite-element method adopted in this work provided more intuitive results compared with analytical modelling[127,128,169], which could then be better compared to the experimental data for subsequent optimization of the experimental design. A key concept proposed in previous studies and confirmed in REF. 170 is the formation of strain-induced charge channels in the p–n junction, which provides an effective means of controlling the photoexcited carriers (FIG. 6). By studying the changes in the band structure, it was suggested that the strain-induced shift of the depletion region and the formation of charge channels at the interface contribute to the mechanically tunable operation of piezo-phototronic devices. The simulation results clearly showed that when the doping concentration in the piezoelectric semiconductor was low (for example, 10^{14}–10^{15} cm^{-3}), the depletion region shifted towards either a p- or n-type region under strain, depending on the strain polarity and the orientation of the polar axis in the piezoelectric material; such changes will result in charge channels for holes or electrons, respectively. The shift of the depletion region, formation of charge channels and related deformation of band profiles at the interface under strain can significantly affect the charge-carrier transport, separation and recombination processes (BOX 2). The dependence of the piezo-phototronic effect on the carrier concentration, geometric factors and material considerations has also been studied theoretically, and fundamental analysis of the piezo-phototronic effect on exciton dissociation at the interface has been recently performed using the finite-element method[171]. These and earlier advances have not only helped to establish a better understanding of piezo-phototronic coupling, but have also provided useful guidance for subsequent experimental work.

Perspective

Despite tremendous progress, much work remains to be done to attain a comprehensive understanding and to realize the full potential of piezotronics and piezo-phototronics. For example, recent theoretical predictions of piezoelectricity in 2D materials[105–108] suggest that atomically thin semiconductors could offer an ideal platform for studying the fundamental piezotronic and piezo-phototronic effects. The coupling between piezoelectricity and semiconducting properties in 2D nanomaterials may be useful in powering nanodevices, adaptive bioprobes, tunable and stretchable electronics, and optoelectronics that are only a few atomic layers thick. Considering their superior mechanical properties[16], atomically thin 2D materials may be preferable to 1D nanomaterials for piezotronic and piezo-phototronic applications in terms of the lifetime and mechanical durability. However, 2D materials are more sensitive than 1D materials to the environmental conditions. For example, the carrier concentration in a 2D material may vary from sample to sample owing to unintentional doping[172]; this can cause variations in the partial screening of the piezoelectric charges and thus affect the piezotronics or piezo-phototronic performance. The use of an additional encapsulation layer, for example, of transferred boron nitride[173] or a dielectric grown by atomic layer deposition[174], is expected to improve the stability of piezotronics and piezo-phototronics based on 2D materials. It is anticipated that most 2D compounds have a non-centrosymmetric monolayer structure and are thus piezoelectric. Therefore, it may be possible to combine the piezoelectric nature of 2D materials with other intriguing properties (for example, thermoelectric[175], superconducting[176] or spintronic[177] properties) in atomically thin crystals.

Mechanical fatigue can compromise device performance during long-term operation. Single-crystalline nanomaterials (for example, ZnO nanowires) possess good mechanical durability. For example, the dynamic fatigue behaviour of ZnO nanowires was studied using *in situ* transmission electron microscopy, whereby the nanowires were shown to be free of fatigue after mechanical deformation at resonance for over 10^{10} cycles[178]; this superior behaviour results from the absence of dislocations and surface stiffening in the nanowire. By contrast, the deposited electrode materials may suffer from poor mechanical stability[179]. Therefore, degradation of the electrode materials and cyclic mechanical deformation of the metal–semiconductor contact are expected to be the main causes of failure of piezotronic and piezo-phototronic devices during long-term cycling. Design and processing strategies that help increase the flexibility (or even stretchability) of the electrode structure (for example, buckled serpentine interconnects[179]) may substantially improve the mechanical stability of as-fabricated piezotronic and piezo-phototronic devices. The development of new electrode materials that can tolerate much larger bending or tensile strain (for example, carbon nanotubes[180] or conducting polymers[181]) may improve mechanical performance. Surprisingly, we still lack a fundamental understanding of how the structure and properties change (if they change at all) in metal–semiconductor contacts in piezotronic and piezo-phototronic devices under dynamic mechanical stimuli. Gaining such knowledge is crucial for the rational design and optimization of piezotronic and piezo-phototronic devices. Finally, the substrate (typically a polymeric material) that supports the active layer of the device and transmits mechanical stimuli to the piezoelectric semiconductors may also experience mechanical fatigue[17,182]. New substrate materials that exhibit larger dynamic ranges of mechanical flexibility or stretchability, and even self-healing characteristics, are expected to have an important role in future piezotronic and piezo-phototronic applications[183].

The incorporation of quantum mechanics into existing models will help to place piezotronics and piezo-phototronics within a complete theoretical framework. Numerical studies hybridizing the existing methods with other approaches (for example, finite-difference time-domain methods) could allow a more

© 2016 Macmillan Publishers Limited. All rights reserved.

precise prediction of the optical behaviour in piezo-phototronic devices. In addition, more sophisticated characterization methods could be adopted. For example, the distribution of piezoelectric polarization could be directly quantified and imaged through Kelvin probe microscopy[184,185], electron holography[186] or soft X-ray scanning photoelectron spectromicroscopy[187]. Such characterization would provide valuable insight and guidelines for the engineering of piezoelectric semiconductors, and motivate subsequent studies aimed at better understanding the coupling between piezotronic or piezo-phototronic effects and materials properties. The fundamental behaviour of charge carriers, including their coupling with piezoelectric polarization, could be better revealed through temperature-controlled experiments, particularly at low temperatures[62,188]. It is possible to tune the piezotronic effect to control quantum transport, spin transport and single-electron transport processes. Last but not least, a materials database would be useful for the scaling and optimization of piezoelectric and ferroelectric devices[189,190].

There are similarities between the piezotronic effect and the modification of the contact potential or band structure by remnant ferroelectric-bound charges in ferroelectric electronics (for example, ferroelectric Schottky diodes[191] or ferroelectric tunnel junctions[192]). Specifically, both involve a shift in the band structure upon the generation of bound polarization charges at the interface, which influences charge transport. However, several important differences distinguish piezotronics from ferroelectric electronics. First, in ferroelectrics, spontaneous polarization occurs upon application of an electric field[191]. The modulation of carrier transport in ferroelectric electronics is thus realized through electrical biasing, which switches the polarization. Second, owing to the nonlinear nature of ferroelectric materials, there is hysteresis in the response of the carrier transport properties to applied stimuli. Third, because of the poor semiconductor properties and lack of mechanical flexibility in most ferroelectric materials, the coupling between electronic transport and polarization charges induced by dynamic strain has not been studied in ferroelectric electronics.

The fields of piezotronics and piezo-phototronics enable the development of new classes of electronics and optoelectronics that can interact with mechanical signals from the environment. In current approaches to implementing devices with similar functionalities, mechanical stimuli need to be converted to electrical signals before the associated electronics or optoelectronics can sense and respond. Moreover, the effect of the mechanical signal in operations of such functional devices needs to be minimized[193,194]. Current devices not only require the complex integration of heterogeneous components, but also lack direct interfacing between the (opto)electronics and the mechanical actuation. Further theoretical and experimental studies are also necessary to improve the stability of device performance and the reliability of the electrode–semiconductor contact, to control the material properties in the piezoelectric semiconductor, and to integrate ordered arrays of piezotronic and piezo-phototronic devices into state-of-the-art electronics and optoelectronics.

Piezotronics and piezo-phototronics have contributed new knowledge to classical semiconductor physics in terms of the coupling between strain-induced interfacial polarization and the band structures and processes of the charge carriers. As a result, there are exciting opportunities in piezoelectric materials research through the incorporation of semiconductor properties (for example, free carriers, junction–contact formation, electronic transport and optical excitation). The understanding and application of this long-overlooked coupling between piezoelectricity and semiconductor properties give rise to new fundamental phenomena and unprecedented device technologies, including superior electronics, optoelectronics and even photoelectrochemical materials.

1. Bonato, P. Wearable sensors and systems from enabling technology to clinical applications. *IEEE Eng. Med. Biol.* **29**, 25–36 (2010).
2. Kim, D. H. *et al.* Epidermal electronics. *Science* **333**, 838–843 (2011).
3. Heng, W., Conrad, N., Wei, L. & Ye, P. D. in *2014 IEEE International Electron Devices Meeting* 9.3.1–9.3.4 (San Francisco, 2014).
4. Muller, R. S., Kamins, T. I. & Chan, M. *Device Electronics for Integrated Circuits* 3rd edn (John Wiley & Sons, 2003).
5. Javey, A., Guo, J., Wang, Q., Lundstrom, M. & Dai, H. J. Ballistic carbon nanotube field-effect transistors. *Nature* **424**, 654–657 (2003).
6. Radisavljevic, B., Radenovic, A., Brivio, J., Giacometti, V. & Kis, A. Single-layer MoS_2 transistors. *Nat. Nanotechnol.* **6**, 147–150 (2011).
7. Cui, Y. & Lieber, C. M. Functional nanoscale electronic devices assembled using silicon nanowire building blocks. *Science* **291**, 851–853 (2001).
8. Baugher, B. W. H., Churchill, H. O. H., Yang, Y. F. & Jarillo-Herrero, P. Optoelectronic devices based on electrically tunable p–n diodes in a monolayer dichalcogenide. *Nat. Nanotechnol.* **9**, 262–267 (2014).
9. Ross, J. S. *et al.* Electrically tunable excitonic light-emitting diodes based on monolayer WSe_2 p–n junctions. *Nat. Nanotechnol.* **9**, 268–272 (2014).
10. Pospischil, A., Furchi, M. M. & Mueller, T. Solar-energy conversion and light emission in an atomic monolayer p–n diode. *Nat. Nanotechnol.* **9**, 257–261 (2014).
11. Novoselov, K. S. *et al.* Electric field effect in atomically thin carbon films. *Science* **306**, 666–669 (2004).
12. Kingon, A. I. & Srinivasan, S. Lead zirconate titanate thin films directly on copper electrodes for ferroelectric, dielectric and piezoelectric applications. *Nat. Mater.* **4**, 233–237 (2005).
13. Ferren, R. A. Advances in polymeric piezoelectric transducers. *Nature* **350**, 26–27 (1991).
14. Chen, C. Q. & Zhu, J. Bending strength and flexibility of ZnO nanowires. *Appl. Phys. Lett.* **90**, 043105 (2007).
15. Li, P. *et al. In situ* transmission electron microscopy investigation on fatigue behavior of single ZnO wires under high-cycle strain. *Nano Lett.* **14**, 480–485 (2014).
16. Bertolazzi, S., Brivio, J. & Kis, A. Stretching and breaking of ultrathin MoS_2. *ACS Nano* **5**, 9703–9709 (2011).
17. Wu, W. Z., Wen, X. N. & Wang, Z. L. Taxel-addressable matrix of vertical-nanowire piezotronic transistors for active and adaptive tactile imaging. *Science* **340**, 952–957 (2013).
18. Pan, C. F. *et al.* High-resolution electroluminescent imaging of pressure distribution using a piezoelectric nanowire LED array. *Nat. Photonics* **7**, 752–758 (2013).
19. Wu, W. Z. *et al.* Piezoelectricity of single-atomic-layer MoS_2 for energy conversion and piezotronics. *Nature* **514**, 470–474 (2014).
20. Qi, J. J. *et al.* Piezoelectric effect in chemical vapour deposition-grown atomic-monolayer triangular molybdenum disulfide piezotronics. *Nat. Commun.* **6**, 7430 (2015).
21. Li, H. X., Yu, Y. H., Starr, M. B., Li, Z. D. & Wang, X. D. Piezotronic-enhanced photoelectrochemical reactions in $Ni(OH)_2$-decorated ZnO photoanodes. *J. Phys. Chem. Lett.* **6**, 3410–3416 (2015).
22. Yang, S. Z. *et al.* The piezotronic effect of zinc oxide nanowires studied by *in situ* TEM. *Adv. Mater.* **24**, 4676–4682 (2012).
23. Baraki, R. *et al.* Varistor piezotronics: mechanically tuned conductivity in varistors. *J. Appl. Phys.* **118**, 085703 (2015).
24. Wang, Z. L. Piezopotential gated nanowire devices: piezotronics and piezo-phototronics. *Nano Today* **5**, 540–552 (2010).
25. Zhou, J. *et al.* Flexible piezotronic strain sensor. *Nano Lett.* **8**, 3035–3040 (2008).
26. Wu, W. Z., Wei, Y. G. & Wang, Z. L. Strain-gated piezotronic logic nanodevices. *Adv. Mater.* **22**, 4711–4715 (2010).
27. Shi, J., Starr, M. B. & Wang, X. D. Band structure engineering at heterojunction interfaces via the piezotronic effect. *Adv. Mater.* **24**, 4683–4691 (2012).

© 2016 Macmillan Publishers Limited. All rights reserved.

28. Wang, Z. L. *Piezotronics and Piezo-Phototronics* (Springer, 2013).
29. Hu, Y. F., Zhang, Y., Chang, Y. L., Snyder, R. L. & Wang, Z. L. Optimizing the power output of a ZnO photocell by piezopotential. *ACS Nano* **4**, 4220–4224 (2010).
30. Hu, Y. F. *et al.* Piezo-phototronic effect on electroluminescence properties of p-type GaN thin films. *Nano Lett.* **12**, 3851–3856 (2012).
31. Yang, Q. *et al.* Largely enhanced efficiency in ZnO nanowire/p-polymer hybridized inorganic/organic ultraviolet light-emitting diode by piezo-phototronic effect. *Nano Lett.* **13**, 607–613 (2013).
32. Wu, W. Z., Pan, C. F., Zhang, Y., Wen, X. N. & Wang, Z. L. Piezotronics and piezo-phototronics — from single nanodevices to array of devices and then to integrated functional system. *Nano Today* **8**, 619–642 (2013).
33. Wang, Z. L. & Wu, W. Z. Piezotronics and piezo-phototronics: fundamentals and applications. *Natl Sci. Rev.* **1**, 62–90 (2014).
34. Kroemer, H. Nobel Lecture. Quasielectric fields and band offsets: teaching electrons new tricks. *Rev. Modern Phys.* **73**, 783–793 (2001).
35. Lin, Y. F. & Jian, W. B. The impact of nanocontact on nanowire based nanoelectronics. *Nano Lett.* **8**, 3146–3150 (2008).
36. Lee, C. H. *et al.* Atomically thin p–n junctions with van der Waals heterointerfaces. *Nat. Nanotechnol.* **9**, 676–681 (2014).
37. Yajima, T. *et al.* Controlling band alignments by artificial interface dipoles at perovskite heterointerfaces. *Nat. Commun.* **6,** 6759 (2015).
38. Qian, F. *et al.* Multi-quantum-well nanowire heterostructures for wavelength-controlled lasers. *Nat. Mater.* **7**, 701–706 (2008).
39. Lopez-Sanchez, O., Lembke, D., Kayci, M., Radenovic, A. & Kis, A. Ultrasensitive photodetectors based on monolayer MoS_2. *Nat. Nanotechnol.* **8**, 497–501 (2013).
40. Habisreutinger, S. N., Schmidt-Mende, L. & Stolarczyk, J. K. Photocatalytic reduction of CO_2 on TiO_2 and other semiconductors. *Angew. Chem. Int. Ed. Engl.* **52**, 7372–7408 (2013).
41. Luo, J. S. *et al.* Water photolysis at 12.3% efficiency via perovskite photovoltaics and Earth-abundant catalysts. *Science* **345**, 1593–1596 (2014).
42. Ozgur, U. *et al.* A comprehensive review of ZnO materials and devices. *J. Appl. Phys.* **98**, 041301 (2005).
43. Wang, Z. L. ZnO nanowire and nanobelt platform for nanotechnology. *Mater. Sci. Eng R–Rep.* **64**, 33–71 (2009).
44. Joo, J., Chow, B. Y., Prakash, M., Boyden, E. S. & Jacobson, J. M. Face-selective electrostatic control of hydrothermal zinc oxide nanowire synthesis. *Nat. Mater.* **10**, 596–601 (2011).
45. Wei, Y. *et al.* Wafer-scale high-throughput ordered growth of vertically aligned ZnO nanowire arrays. *Nano Lett.* **10**, 3414–3419 (2010).
46. Zhou, J. *et al.* Piezoelectric-potential-control led polarity-reversible Schottky diodes and switches of ZnO wires. *Nano Lett.* **8**, 3973–3977 (2008).
47. Fei, P. *et al.* Piezoelectric potential gated field-effect transistor based on a free-standing ZnO wire. *Nano Lett.* **9**, 3435–3439 (2009).
48. Xu, Z. *et al.* Lateral piezopotential-gated field-effect transistor of ZnO nanowires. *Nano Energy* **13**, 233–239 (2015).
49. Wang, X. *et al.* Piezoelectric field effect transistor and nanoforce sensor based on a single ZnO nanowire. *Nano Lett.* **6**, 2768–2772 (2006).
50. Liu, W. H., Lee, M., Ding, L., Liu, J. & Wang, Z. L. Piezopotential gated nanowire–nanotube hybrid field-effect transistor. *Nano Lett.* **10**, 3084–3089 (2010).
51. Sun, Q. *et al.* Active matrix electronic skin strain sensor based on piezopotential-powered graphene transistors. *Adv. Mater.* **27**, 3411–3417 (2015).
52. Chen, L. *et al.* Strain-gated field effect transistor of a MoS_2–ZnO 2D–1D hybrid structure. *ACS Nano* **10**, 1546–1551 (2015).
53. Han, W. H. *et al.* Strain-gated piezotronic transistors based on vertical zinc oxide nanowires. *ACS Nano* **6**, 3760–3766 (2012).
54. Zhou, Y. S. *et al.* Vertically aligned CdSe nanowire arrays for energy harvesting and piezotronic devices. *ACS Nano* **6**, 6478–6482 (2012).
55. Yu, R., Wu, W., Ding, Y. & Wang, Z. L. GaN nanobelt-based strain-gated piezotronic logic devices and computation. *ACS Nano* **7**, 6403–6409 (2013).
56. Zhu, R. & Yang, R. S. Separation of the piezotronic and piezoresistive effects in a zinc oxide nanowire. *Nanotechnology* **25**, 345702 (2014).
57. Wu, W. Z. & Wang, Z. L. Piezotronic nanowire-based resistive switches as programmable electromechanical memories. *Nano Lett.* **11**, 2779–2785 (2011).
58. Pradel, K. C. *et al.* Piezotronic effect in solution-grown p-type ZnO nanowires and films. *Nano Lett.* **13**, 2647–2653 (2013).
59. Zhang, J. & Meguid, S. A. On the piezoelectric potential of gallium nitride nanotubes. *Nano Energy* **12**, 322–330 (2015).
60. Yu, R. M. *et al.* Piezotronic effect on the transport properties of GaN nanobelts for active flexible electronics. *Adv. Mater.* **24**, 3532–3537 (2012).
61. Liu, H. F., Liu, W., Chua, S. J. & Chi, D. Z. Fabricating high-quality GaN-based nanobelts by strain-controlled cracking of thin solid films for application in piezotronics. *Nano Energy* **1**, 316–321 (2012).
62. Yu, R. M. *et al.* Temperature dependence of the piezophototronic effect in CdS nanowires. *Adv. Funct. Mater.* **25**, 5277–5284 (2015).
63. Rai, S. C. *et al.* Enhanced broad band photodetection through piezo-phototronic effect in CdSe/ZnTe core/shell nanowire array. *Adv. Electron. Mater.* **1**, 1400050 (2015).
64. Li, X. *et al.* Remarkable and crystal-structure-dependent piezoelectric and piezoresistive effects of InAs nanowires. *Adv. Mater.* **27**, 2852–2858 (2015).
65. Ku, N. J., Huang, J. H., Wang, C. H., Fang, H. C. & Liu, C. P. Crystal face-dependent nanopiezotronics of an obliquely aligned InN nanorod array. *Nano Lett.* **12**, 562–568 (2012).
66. Wu, J. M., Chen, K. H., Zhang, Y. & Wang, Z. L. A self-powered piezotronic strain sensor based on single $ZnSnO_3$ microbelts. *RSC Adv.* **3**, 25184–25189 (2013).
67. Wu, J. M. *et al.* Ultrahigh sensitive piezotronic strain sensors based on a $ZnSnO_3$ nanowire/microwire. *ACS Nano* **6**, 4369–4374 (2012).
68. Hou, T.-C. *et al.* Nanogenerator based on zinc blende CdTe micro/nanowires. *Nano Energy* **2**, 387–393 (2013).
69. Chen, Y. Y., Wang, C. H., Chen, G. S., Li, Y. C. & Liu, C. P. Self-powered n-$Mg_xZn_{1-x}O$/p-Si photodetector improved by alloying-enhanced piezopotential through piezo-phototronic effect. *Nano Energy* **11**, 533–539 (2015).
70. Wang, C. H., Lai, K. Y., Li, Y. C., Chen, Y. C. & Liu, C. P. Ultrasensitive thin-film-based $Al_xGa_{1-x}N$ piezotronic strain sensors via alloying-enhanced piezoelectric potential. *Adv. Mater.* **27**, 6289–6295 (2015).
71. Liao, X. Q. *et al.* Enhanced performance of ZnO piezotronic pressure sensor through electron-tunneling modulation of MgO nano layer. *ACS Appl. Mater. Interfaces* **7**, 1602–1607 (2015).
72. Zhang, Z., Liao, Q. L., Yu, Y. H., Wang, X. D. & Zhang, Y. Enhanced photoresponse of ZnO nanorods-based self-powered photodetector by piezotronic interface engineering. *Nano Energy* **9**, 237–244 (2014).
73. Liao, Q. L., Liang, M. Y., Zhang, Z., Zhang, G. J. & Zhang, Y. Strain-modulation and service behavior of Au–MgO–ZnO ultraviolet photodetector by piezo-phototronic effect. *Nano Res.* **8**, 3772–3779 (2015).
74. Pradel, K. C., Wu, W., Ding, Y. & Wang, Z. L. Solution-derived ZnO homojunction nanowire films on wearable substrates for energy conversion and self-powered gesture recognition. *Nano Lett.* **14**, 6897–6905 (2014).
75. Lin, P. *et al.* Enhanced photoresponse of Cu_2O/ZnO heterojunction with piezo-modulated interface engineering. *Nano Res.* **7**, 860–868 (2014).
76. Jalali, N. *et al.* Improved performance of p–n junction-based ZnO nanogenerators through CuSCN-passivation of ZnO nanorods. *J. Mater. Chem. A* **2**, 10945–10951 (2014).
77. Lin, P. *et al.* Self-powered UV photosensor based on PEDOT:PSS/ZnO micro/nanowire with strain-modulated photoresponse. *ACS Appl. Mater. Interfaces* **5**, 3671–3676 (2013).
78. Yang, Y. *et al.* Piezotronic effect on the output voltage of P3HT/ZnO micro/nanowire heterojunction solar cells. *Nano Lett.* **11**, 4812–4817 (2011).
79. Araneo, R. & Falconi, C. Lateral bending of tapered piezo-semiconductive nanostructures for ultra-sensitive mechanical force to voltage conversion. *Nanotechnology* **24**, 265707 (2013).
80. Zhang, R. Y. *et al.* Piezoelectric gated ZnO nanowire diode studied by *in situ* TEM probing. *Nano Energy* **3**, 10–15 (2014).
81. Zhao, Z. F. *et al.* Piezotronic effect in polarity-controlled GaN nanowires. *ACS Nano* **9**, 8578–8583 (2015).
82. Wang, X. *et al.* Temperature dependence of the piezotronic and piezophototronic effects in *a*-axis GaN nanobelts. *Adv. Mater.* **27**, 8067–8074 (2015).
83. Yu, R. *et al.* Piezotronic effect in strain-gated transistor of *a*-axis GaN nanobelt. *ACS Nano* **9**, 9822–9829 (2015).
84. Zhang, Z. *et al.* Highly efficient piezotronic strain sensors with symmetrical Schottky contacts on the monopolar surface of ZnO nanobelts. *Nanoscale* **7**, 1796–1801 (2015).
85. Wu, W., Pan, C., Zhang, Y., Wen, X. & Wang, Z. L. Piezotronics and piezo-phototronics — from single nanodevices to array of devices and then to integrated functional system. *Nano Today* **8**, 619–642 (2013).
86. Xing, L. L. *et al.* Realizing room-temperature self-powered ethanol sensing of Au/ZnO nanowire arrays by coupling the piezotronics effect of ZnO and the catalysis of noble metal. *Appl. Phys. Lett.* **104**, 013109 (2014).
87. Han, Y. *et al.* Piezotronic effect enhanced nanowire sensing of H_2O_2 released by cells. *Nano Energy* **13**, 405–413 (2015).
88. Liao, Q. L. *et al.* Carbon fiber–ZnO nanowire hybrid structures for flexible and adaptable strain sensors. *Nanoscale* **5**, 12350–12355 (2013).
89. Yu, R., Pan, C., Chen, J., Zhu, G. & Wang, Z. L. Enhanced performance of a ZnO nanowire-based self-powered glucose sensor by piezotronic effect. *Adv. Funct. Mater.* **23**, 5868–5874 (2013).
90. Pan, C. F., Yu, R. M., Niu, S. M., Zhu, G. & Wang, Z. L. Piezotronic effect on the sensitivity and signal level of Schottky contacted proactive micro/nanowire nanosensors. *ACS Nano* **7**, 1803–1810 (2013).
91. Yu, R. M., Pan, C. F. & Wang, Z. L. High performance of ZnO nanowire protein sensors enhanced by the piezotronic effect. *Energ Environ. Sci.* **6**, 494–499 (2013).
92. Niu, S. *et al.* Enhanced performance of flexible ZnO nanowire based room-temperature oxygen sensors by piezotronic effect. *Adv. Mater.* **25**, 3701–3706 (2013).
93. Wang, N. *et al.* Piezotronic-effect enhanced drug metabolism and sensing on a single ZnO nanowire surface with the presence of human cytochrome P450. *ACS Nano* **9**, 3159–3168 (2015).
94. Zhou, R. R., Hu, G. F., Yu, R. M., Pan, C. F. & Wang, Z. L. Piezotronic effect enhanced detection of flammable/toxic gases by ZnO micro/nanowire sensors. *Nano Energy* **12**, 588–596 (2015).
95. Hu, G. F. *et al.* Piezotronic effect enhanced Schottky-contact ZnO micro/nanowire humidity sensors. *Nano Res.* **7**, 1083–1091 (2014).
96. Duerloo, K. A. N., Ong, M. T. & Reed, E. J. Intrinsic piezoelectricity in two-dimensional materials. *J. Phys. Chem. Lett.* **3**, 2871–2876 (2012).
97. Ahmadpoor, F. & Sharma, P. Flexoelectricity in two-dimensional crystalline and biological membranes. *Nanoscale* **7**, 16555–16570 (2015).
98. Blonsky, M. N., Zhuang, H. L., Singh, A. K. & Hennig, R. G. *Ab initio* prediction of piezoelectricity in two-dimensional materials. *ACS Nano* **9**, 9885–9891 (2015).
99. Mak, K. F., Lee, C., Hone, J., Shan, J. & Heinz, T. F. Atomically thin MoS_2: a new direct-gap semiconductor. *Phys. Rev. Lett.* **105**, 136805 (2010).
100. Castellanos-Gomez, A. *et al.* Elastic properties of freely suspended MoS_2 nanosheets. *Adv. Mater.* **24**, 772–775 (2012).
101. Manzeli, S., Allain, A., Ghadimi, A. & Kis, A. Piezoresistivity and strain-induced band gap tuning in atomically thin MoS_2. *Nano Lett.* **15**, 5330–5335 (2015).
102. Conley, H. J. *et al.* Bandgap engineering of strained monolayer and bilayer MoS_2. *Nano Lett.* **13**, 3626–3630 (2013).
103. van der Zande, A. M. *et al.* Grains and grain boundaries in highly crystalline monolayer molybdenum disulphide. *Nat. Mater.* **12**, 554–561 (2013).
104. Zhu, H. Y. *et al.* Observation of piezoelectricity in free-standing monolayer MoS_2. *Nat. Nanotechnol.* **10**, 151–155 (2015).
105. Fei, R. X., Li, W. B., Li, J. & Yang, L. Giant piezoelectricity of monolayer group IV monochalcogenides: SnSe, SnS, GeSe, and GeS. *Appl. Phys. Lett.* **107**, 173104 (2015).
106. Gomes, L. C., Carvalho, A. & Neto, A. H. C. Enhanced piezoelectricity and modified dielectric screening of two-dimensional group-IV monochalcogenides. *Phys. Rev. B* **92,** 214103 (2015).

© 2016 Macmillan Publishers Limited. All rights reserved.

107. Li, W. B. & Li, J. Piezoelectricity in two-dimensional group-III monochalcogenides. *Nano Res.* **8**, 3796–3802 (2015).
108. Alyoruk, M. M., Aierken, Y., Cakir, D., Peeters, F. M. & Sevik, C. Promising piezoelectric performance of single layer transition-metal dichalcogenides and dioxides. *J. Phys. Chem. C* **119**, 23231–23237 (2015).
109. Wen, X. N., Wu, W. Z., Ding, Y. & Wang, Z. L. Piezotronic effect in flexible thin-film based devices. *Adv. Mater.* **25**, 3371–3379 (2013).
110. Xue, F. *et al.* Piezotronic effect on ZnO nanowire film based temperature sensor. *ACS Appl. Mater. Interfaces* **6**, 5955–5961 (2014).
111. Baraki, R., Novak, N., Froemling, T., Granzow, T. & Roedel, J. Bulk ZnO as piezotronic pressure sensor. *Appl. Phys. Lett.* **105,** 111604 (2014).
112. Raidl, N., Supancic, P., Danzer, R. & Hofstaetter, M. Piezotronically modified double Schottky barriers in ZnO varistors. *Adv. Mater.* **27**, 2031–2035 (2015).
113. Zhang, Y., Liu, Y. & Wang, Z. L. Fundamental theory of piezotronics. *Adv. Mater.* **23**, 3004–3013 (2011).
114. Araneo, R. *et al.* Current–voltage characteristics of ZnO nanowires under uniaxial loading. *IEEE Trans. Nanotechnol.* **13**, 724–735 (2014).
115. Mitin, V. V., Kochelap, V. A. & Stroscio, M. A. *Introduction to Nanoelectronics: Science, Nanotechnology, Engineering, and Applications* (Cambridge University Press, 2008).
116. Liu, W., Zhang, A., Zhang, Y. & Lin Wang, Z. First principle simulations of piezotronic transistors. *Nano Energy* **14**, 355–363 (2015).
117. Jin, L. S. & Li, L. J. Quantum simulation of ZnO nanowire piezotronics. *Nano Energy* **15**, 776–781 (2015).
118. Zhang, G. H., Zheng, Y. & Wang, B. Dissimilar-electrodes-induced asymmetric characteristic and diode effect of current transport in zinc oxide tunnel junctions. *J. Appl. Phys.* **114**, 044111 (2013).
119. Zhang, G. H., Luo, X., Zheng, Y. & Wang, B. A. Giant piezoelectric resistance effect of nanoscale zinc oxide tunnel junctions: first principles simulations. *Phys. Chem. Chem. Phys.* **14**, 7051–7058 (2012).
120. Zhu, J., Chen, W. J., Zhang, G. H. & Zheng, Y. Exponential size-dependent tunability of strain on the transport behavior in ZnO tunnel junctions: an *ab initio* study. *Phys. Chem. Chem. Phys.* **17**, 25583–25592 (2015).
121. Rinaldi, A., Araneo, R., Celozzi, S., Pea, M. & Notargiacomo, A. The clash of mechanical and electrical size-effects in ZnO nanowires and a double power law approach to elastic strain engineering of piezoelectric and piezotronic devices. *Adv. Mater.* **26**, 5976–5985 (2014).
122. Araneo, R. *et al.* Thermal-electric model for piezoelectric ZnO nanowires. *Nanotechnology* **26**, 265402 (2015).
123. Hu, G. W. *et al.* Piezotronic transistors in nonlinear circuit: model and simulation. *Sci. China: Technol. Sci.* **58**, 1348–1354 (2015).
124. Al-Zahrani, H. Y. S., Pal, J., Migliorato, M. A., Tse, G. & Yu, D. Piezoelectric field enhancement in III–V core–shell nanowires. *Nano Energy* **14**, 382–391 (2015).
125. Liu, W., Zhang, A. H., Zhang, Y. & Wang, Z. L. Density functional studies on edge-contacted single-layer MoS_2 piezotronic transistors. *Appl. Phys. Lett.* **107**, 083105 (2015).
126. Bhattacharya, P. *Semiconductor Optoelectronic Devices* 2nd edn (Prentice Hall, 1997).
127. Zhang, Y., Yang, Y. & Wang, Z. L. Piezo-phototronics effect on nano/microwire solar cells. *Energy Environ. Sci.* **5**, 6850–6856 (2012).
128. Liu, Y., Yang, Q., Zhang, Y., Yang, Z. Y. & Wang, Z. L. Nanowire piezo-phototronic photodetector: theory and experimental design. *Adv. Mater.* **24**, 1410–1417 (2012).
129. Yang, Q., Wang, W. H., Xu, S. & Wang, Z. L. Enhancing light emission of ZnO microwire-based diodes by piezo-phototronic effect. *Nano Lett.* **11**, 4012–4017 (2011).
130. Hu, Y., Chang, Y., Fei, P., Snyder, R. L. & Wang, Z. L. Designing the electric transport characteristics of ZnO micro/nanowire devices by coupling piezoelectric and photoexcitation effects. *ACS Nano* **4**, 1234–1240 (2010).
131. Yang, Q. *et al.* Enhancing sensitivity of a single ZnO micro-/nanowire photodetector by piezo-phototronic effect. *ACS Nano* **4**, 6285–6291 (2010).
132. Boxberg, F., Sondergaard, N. & Xu, H. Q. Photovoltaics with piezoelectric core–shell nanowires. *Nano Lett.* **10**, 1108–1112 (2010).
133. Pan, C. F. *et al.* Enhanced Cu_2S/CdS coaxial nanowire solar cells by piezo-phototronic effect. *Nano Lett.* **12**, 3302–3307 (2012).
134. Shi, J., Zhao, P. & Wang, X. D. Piezoelectric-polarization-enhanced photovoltaic performance in depleted-heterojunction quantum-dot solar cells. *Adv. Mater.* **25**, 916–921 (2013).
135. Wang, Z. Z. *et al.* Enhancing sensitivity of force sensor based on a ZnO tetrapod by piezo-phototronic effect. *Appl. Phys. Lett.* **103**, 143125 (2013).
136. Zhang, F., Ding, Y., Zhang, Y., Zhang, X. L. & Wang, Z. L. Piezo-phototronic effect enhanced visible and ultraviolet photodetection using a ZnO–CdS core–shell micro/nanowire. *ACS Nano* **6**, 9229–9236 (2012).
137. Dong, L. *et al.* Piezo-phototronic effect of CdSe nanowires. *Adv. Mater.* **24**, 5470–5475 (2012).
138. Shi, J. *et al.* Interface engineering by piezoelectric potential in ZnO-based photoelectrochemical anode. *Nano Lett.* **11**, 5587–5593 (2011).
139. Starr, M. B., Shi, J. & Wang, X. D. Piezopotential-driven redox reactions at the surface of piezoelectric materials. *Angew. Chem. Int. Ed. Engl.* **51**, 5962–5966 (2012).
140. Liao, Z. M. *et al.* Strain induced exciton fine-structure splitting and shift in bent ZnO microwires. *Sci. Rep.* **2**, 452 (2012).
141. Han, X. B. *et al.* Electronic and mechanical coupling in bent ZnO nanowires. *Adv. Mater.* **21**, 4937–4941 (2009).
142. Wei, B. *et al.* Size-dependent bandgap modulation of ZnO nanowires by tensile strain. *Nano Lett.* **12**, 4595–4599 (2012).
143. Dietrich, C. P. *et al.* Strain distribution in bent ZnO microwires. *Appl. Phys. Lett.* **98**, 031105 (2011).
144. Fu, X. W., Liao, Z. M., Liu, R., Xu, J. & Yu, D. P. Size-dependent correlations between strain and phonon frequency in individual ZnO nanowires. *ACS Nano* **7**, 8891–8898 (2013).
145. Fu, X. W. *et al.* Tailoring exciton dynamics by elastic strain-gradient in semiconductors. *Adv. Mater.* **26**, 2572–2579 (2014).
146. Xu, S. G., Guo, W. H., Du, S. W., Loy, M. M. T. & Wang, N. Piezotronic effects on the optical properties of ZnO nanowires. *Nano Lett.* **12**, 5802–5807 (2012).
147. Lu, S. N. *et al.* Piezotronic interface engineering on ZnO/Au-based Schottky junction for enhanced photoresponse of a flexible self-powered UV detector. *ACS Appl. Mater. Interfaces* **6**, 14116–14122 (2014).
148. Peng, M. *et al.* Flexible self-powered GaN ultraviolet photoswitch with piezo-phototronic effect enhanced on/off ratio. *ACS Nano* **10**, 1572–1579 (2016).
149. Chen, J. X. *et al.* Strain-enhanced cable-type 3D UV photodetecting of ZnO nanowires on a Ni wire by coupling of piezotronics effect and pn junction. *Opt. Express* **22**, 3661–3668 (2014).
150. Luo, Y. M. *et al.* Piezoelectric effect enhancing decay time of p-NiO/n-ZnO ultraviolet photodetector. *Appl. Surf. Sci.* **361**, 157–161 (2016).
151. Wang, Z. N. *et al.* Piezo-phototronic UV/visible photosensing with optical-fiber-nanowire hybridized structures. *Adv. Mater.* **27**, 1553–1560 (2015).
152. Rai, S. C. *et al.* Piezo-phototronic effect enhanced UV/visible photodetector based on fully wide band gap type-II ZnO/ZnS core/shell nanowire array. *ACS Nano* **9**, 6419–6427 (2015).
153. Wang, Z. *et al.* Optimizing performance of silicon-based p–n junction photodetectors by the piezo-phototronic effect. *ACS Nano* **8**, 12866–12873 (2014).
154. Li, X. Y. *et al.* Enhancing light emission of ZnO-nanofilm/Si-micropillar heterostructure arrays by piezo-phototronic effect. *Adv. Mater.* **27**, 4447–4453 (2015).
155. Wang, C. F. *et al.* Enhanced emission intensity of vertical aligned flexible ZnO nanowire/p-polymer hybridized LED array by piezo-phototronic effect. *Nano Energy* **14**, 364–371 (2015).
156. Bao, R. R. *et al.* Flexible and controllable piezo-phototronic pressure mapping sensor matrix by ZnO NW/p-polymer LED array. *Adv. Funct. Mater.* **25**, 2884–2891 (2015).
157. Du, C. H. *et al.* Piezo-phototronic effect controlled dual-channel visible light communication (PVLC) using InGaN/GaN multiquantum well nanopillars. *Small* **11**, 6071–6077 (2015).
158. Guo, Z. *et al.* Large-scale horizontally aligned ZnO microrod arrays with controlled orientation, periodic distribution as building blocks for chip-in piezo-phototronic LEDs. *Small* **11**, 438–445 (2015).
159. Nozaki, K. *et al.* Sub-femtojoule all-optical switching using a photonic-crystal nanocavity. *Nat. Photonics* **4**, 477–483 (2010).
160. Peng, M. Z. *et al.* High-resolution dynamic pressure sensor array based on piezo-phototronic effect tuned photoluminescence imaging. *ACS Nano* **9**, 3143–3150 (2015).
161. Zhang, Y. *et al.* Piezo-phototronic effect-induced dual-mode light and ultrasound emissions from ZnS:Mn/PMN–PT thin-film structures. *Adv. Mater.* **24**, 1729–1735 (2012).
162. Chen, L., Wong, M. C., Bai, G. X., Jie, W. J. & Hao, J. H. White and green light emissions of flexible polymer composites under electric field and multiple strains. *Nano Energy* **14**, 372–381 (2015).
163. Wang, X. *et al.* Dynamic pressure mapping of personalized handwriting by a flexible sensor matrix based on the mechanoluminescence process. *Adv. Mater.* **27**, 2324–2331 (2015).
164. Wong, M. C., Chen, L., Tsang, M. K., Zhang, Y. & Hao, J. H. Magnetic-induced luminescence from flexible composite laminates by coupling magnetic field to piezophotonic effect. *Adv. Mater.* **27**, 4488–4495 (2015).
165. Tsang, M.-K., Bai, G. & Hao, J. Stimuli responsive upconversion luminescence nanomaterials and films for various applications. *Chem. Soc. Rev.* **44**, 1585–1607 (2015).
166. Wang, L. *et al.* Piezotronic effect enhanced photocatalysis in strained anisotropic ZnO/TiO_2 nanoplatelets via thermal stress. *ACS Nano* **10**, 2636–2643 (2016).
167. Yu, R. *et al.* Piezo-phototronic boolean logic and computation using photon and strain dual-gated nanowire transistors. *Adv. Mater.* **27**, 940–947 (2015).
168. Wen, X., Wu, W. & Wang, Z. L. Effective piezo-phototronic enhancement of solar cell performance by tuning material properties. *Nano Energy* **2**, 1093–1100 (2013).
169. Zhang, Y. & Wang, Z. L. Theory of piezo-phototronics for light-emitting diodes. *Adv. Mater.* **24**, 4712–4718 (2012).
170. Liu, Y. *et al.* Theoretical study of piezo-phototronic nano-LEDs. *Adv. Mater.* **26**, 7209–7216 (2014).
171. Kim, S. Piezoelectric effects on the exciton dissociation rate in organic–inorganic hybrid systems. *Integr. ferroelectr.* **167**, 69–77 (2015).
172. Dean, C. R. *et al.* Boron nitride substrates for high-quality graphene electronics. *Nat. Nanotechnol.* **5**, 722–726 (2010).
173. Meric, I. *et al.* Graphene field-effect transistors based on boron-nitride dielectrics. *Proc. IEEE* **101**, 1609–1619 (2013).
174. Zhu, H. *et al.* Al_2O_3 on black phosphorus by atomic layer deposition: an *in situ* interface study. *ACS Appl. Mater. Interfaces* **7**, 13038–13043 (2015).
175. Kayyalha, M. & Chen, Y. P. in *72nd Device Research Conference* 101–102 (California, 2014).
176. Xi, X. *et al.* Strongly enhanced charge-density-wave order in monolayer $NbSe_2$. *Nat. Nanotechnol.* **10**, 765–769 (2015).
177. Xiao, D., Liu, G.-B., Feng, W., Xu, X. & Yao, W. Coupled spin and valley physics in monolayers of MoS_2 and other group-VI dichalcogenides. *Phys. Rev. Lett.* **108**, 196802 (2012).
178. Gao, Z., Ding, Y., Lin, S., Hao, Y. & Wang, Z. L. Dynamic fatigue studies of ZnO nanowires by *in-situ* transmission electron microscopy. *Phys. Status Solidi RRL* **3**, 260–262 (2009).
179. Rogers, J. A., Someya, T. & Huang, Y. Materials and mechanics for stretchable electronics. *Science* **327**, 1603–1607 (2010).
180. Sekitani, T. *et al.* A rubberlike stretchable active matrix using elastic conductors. *Science* **321**, 1468–1472 (2008).
181. Vosgueritchian, M., Lipomi, D. J. & Bao, Z. Highly conductive and transparent PEDOT:PSS films with a fluorosurfactant for stretchable and flexible transparent electrodes. *Adv. Funct. Mater.* **22**, 421–428 (2012).
182. Yang, R., Qin, Y., Dai, L. & Wang, Z. L. Power generation with laterally packaged piezoelectric fine wires. *Nat. Nanotechnol.* **4**, 34–39 (2009).
183. Benight, S. J., Wang, C., Tok, J. B. H. & Bao, Z. Stretchable and self-healing polymers and devices for electronic skin. *Prog. Polym. Sci.* **38**, 1961–1977 (2013).
184. Bayerl, D. J. & Wang, X. Three-dimensional kelvin probe microscopy for characterizing in-plane piezoelectric potential of laterally deflected ZnO micro-/nanowires. *Adv. Funct. Mater.* **22**, 652–660 (2012).

© 2016 Macmillan Publishers Limited. All rights reserved.

185. Geng, D., Pook, A. & Wang, X. Mapping of strain-piezopotential relationship along bent zinc oxide microwires. *Nano Energy* **2**, 1225–1231 (2013).
186. Song, K. *et al.* Correlative high-resolution mapping of strain and charge density in a strained piezoelectric multilayer. *Adv. Mater. Interfaces* **2,** 1400281 (2015).
187. Wang, C. L. *et al.* Imaging and characterization of piezoelectric potential in a single bent ZnO microwire. *Appl. Phys. Lett.* **105,** 123115 (2014).
188. Hu, Y. F. *et al.* Temperature dependence of the piezotronic effect in ZnO nanowires. *Nano Lett.* **13**, 5026–5032 (2013).
189. Li, H. *et al.* Enhanced ferroelectric-nanocrystal-based hybrid photocatalysis by ultrasonic-wave-generated piezophototronic effect. *Nano Lett.* **15**, 2372–2379 (2015).
190. Yang, W. G. *et al.* Ferroelectric polarization-enhanced photoelectrochemical water splitting in TiO_2–$BaTiO_3$ core–shell nanowire photoanodes. *Nano Lett.* **15**, 7574–7580 (2015).
191. Blom, P. W. M., Wolf, R. M., Cillessen, J. F. M. & Krijn, M. Ferroelectric Schottky diode. *Phys. Rev. Lett.* **73**, 2107–2110 (1994).
192. Kohlstedt, H., Pertsev, N. A., Contreras, J. R. & Waser, R. Theoretical current–voltage characteristics of ferroelectric tunnel junctions. *Phys. Rev. B* **72**, 125341 (2005).
193. Tao, H. *et al.* Silk-based resorbable electronic devices for remotely controlled therapy and *in vivo* infection abatement. *Proc. Natl Acad. Sci. USA* **111**, 17385–17389 (2014).
194. Tee, B. C. K. *et al.* A skin-inspired organic digital mechanoreceptor. *Science* **350**, 313–316 (2015).
195. Wang, X. D. Piezotronics: a new field of strain-engineered functional semiconductor devices. *Am. Ceram. Soc. Bull.* **92**, 18–23 (2013).
196. Rhoderick, E. H. & Williams, R. H. *Metal–Semiconductor Contacts* 2nd edn (Clarendon Press, 1988).
197. Wang, Z. L. Progress in piezotronics and piezo-phototronics. *Adv. Mater.* **24**, 4632–4646 (2012).
198. Lu, S. N. *et al.* Influence of the carrier concentration on the piezotronic effect in a ZnO/Au Schottky junction. *Nanoscale* **7**, 4461–4467 (2015).
199. Xue, F. *et al.* Influence of external electric field on piezotronic effect in ZnO nanowires. *Nano Res.* **8**, 2390–2399 (2015).
200. Lee, K. Y. *et al.* Depletion width engineering via surface modification for high performance semiconducting piezoelectric nanogenerators. *Nano Energy* **8**, 165–173 (2014).
201. Wang, C. H. *et al.* Effects of free carriers on piezoelectric nanogenerators and piezotronic devices made of GaN nanowire arrays. *Small* **10**, 4718–4725 (2014).
202. Hu, Y., Lin, L., Zhang, Y. & Wang, Z. L. Replacing a battery by a nanogenerator with 20V output. *Adv. Mater.* **24**, 110–114 (2012).
203. Kang, J. H., Liu, W., Sarkar, D., Jena, D. & Banerjee, K. Computational study of metal contacts to monolayer transition-metal dichalcogenide semiconductors. *Phys. Rev. X* **4,** 031005 (2014).
204. Feng, X. L., Zhang, Y. & Wang, Z. L. Theoretical study of piezotronic heterojunction. *Sci. China: Technol. Sci.* **56**, 2615–2621 (2013).

Acknowledgements
The authors are thankful for the support from the US Department of Energy, Office of Basic Energy Sciences (Award DE-FG02-07ER46394), the National Science Foundation (DMR-1505319), and the Thousand Talents program for a pioneer researcher and his innovation team, China. W.Z.W. is grateful to the College of Engineering and School of Industrial Engineering at Purdue University for the start-up support.

Competing interests statement
The authors declare no competing interests.

© 2016 Macmillan Publishers Limited. All rights reserved.